Statistical properties of undulator radiation

Ihar Lobach (UChicago/Fermilab → Argonne National Laboratory)

IBIC 2022 MO2I4

Faraday Cup Award

Monday, September 12th, 2022

I. Lobach, E. Angelico, UChicago, S. Nagaitsev, G. Stancari, V. Lebedev, A. Romanov, A. Valishev, J. Santucci, Fermilab, A. Halavanau, Z. Huang, V. Yakimenko, SLAC, A. Murokh, Radiabeam, K. J. Kim, ANL, T. Shaftan, BNL

The work is supported by the U.S. Department of Energy, Office of Science, Office of Basic Energy Sciences, under Contract No. DE-AC02-06CH11357.

Fermilab's Integrable Optics Test Accelerator (IOTA)

- First beam Aug 21, 2018

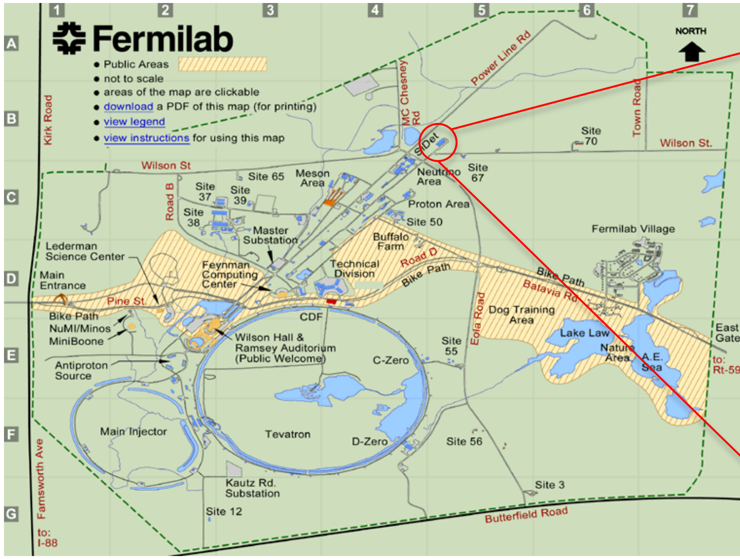

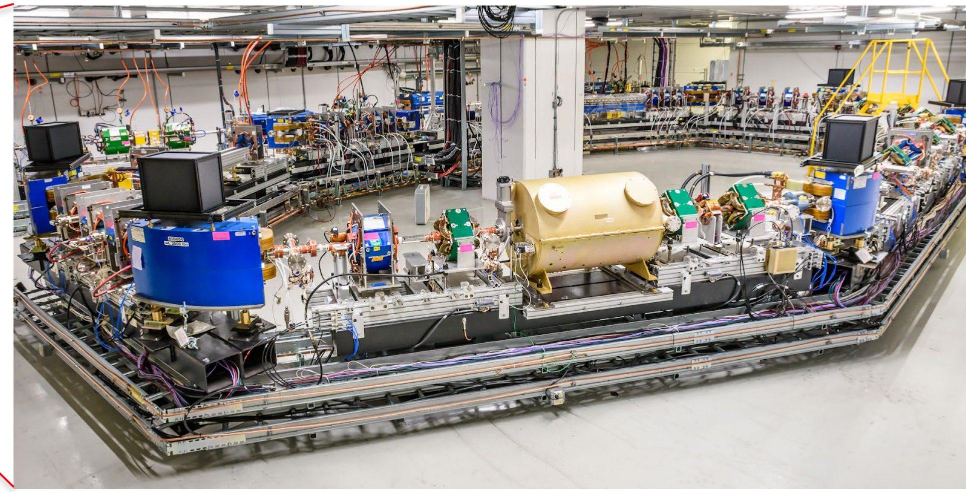

Primary purpose: accelerator science and technology research (not production of radiation for users)

- Particles: electrons/protons
- Main experiments:
  - Nonlinear beam optics
  - Optical stochastic cooling

Circumference: 40 m (133 ns)

Electron energy: 100 MeV

*plus some measurements at 150 MeV

Parameters of the undulator in IOTA

Many thanks to our collaborators from SLAC for providing the undulator

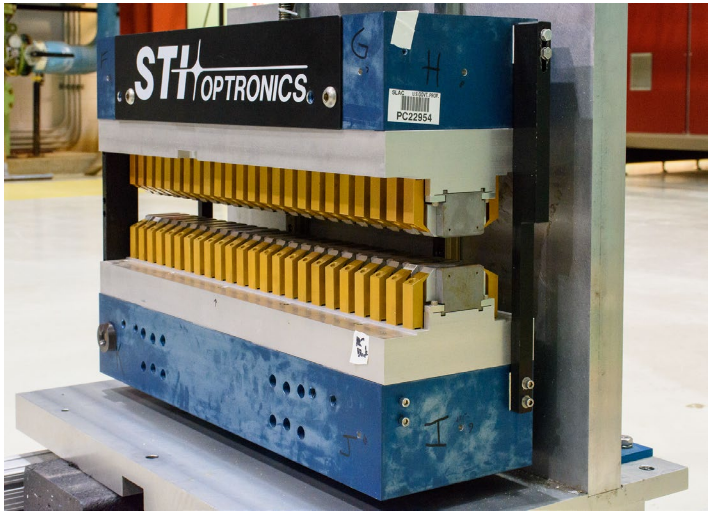

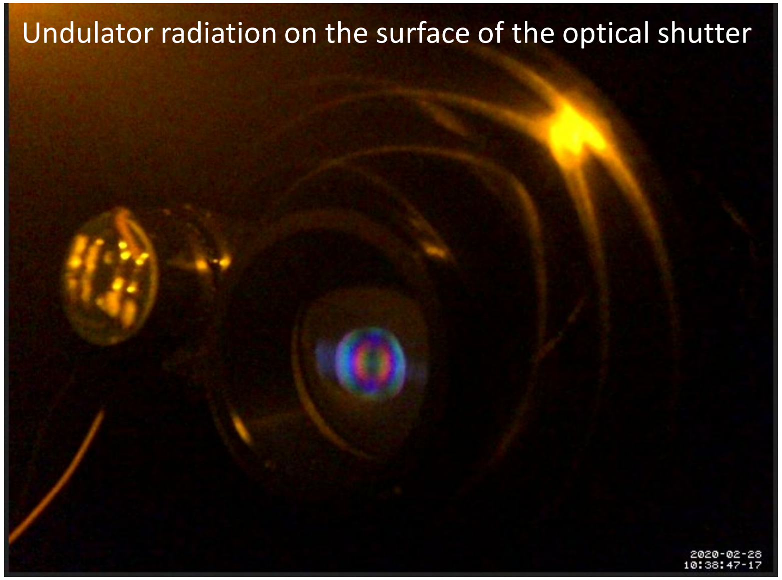

Undulator radiation on the surface of the optical shutter

Undulator:

- Number of periods: $N_{\mathrm{u}} = 10.5$
- Undulator period length: $\lambda_{\mathrm{u}} = 55\ \mathrm{mm}$
- Undulator parameter (peak): $K_{\mathrm{u}} = 1$
- Fundamental of radiation: 1.1 um
- Second harmonic: visible light

$$K_{\mathrm{u}} = \frac{eB\lambda_{\mathrm{u}}}{2\pi m_e c}$$

@100MeV

Layout of the undulator section in IOTA

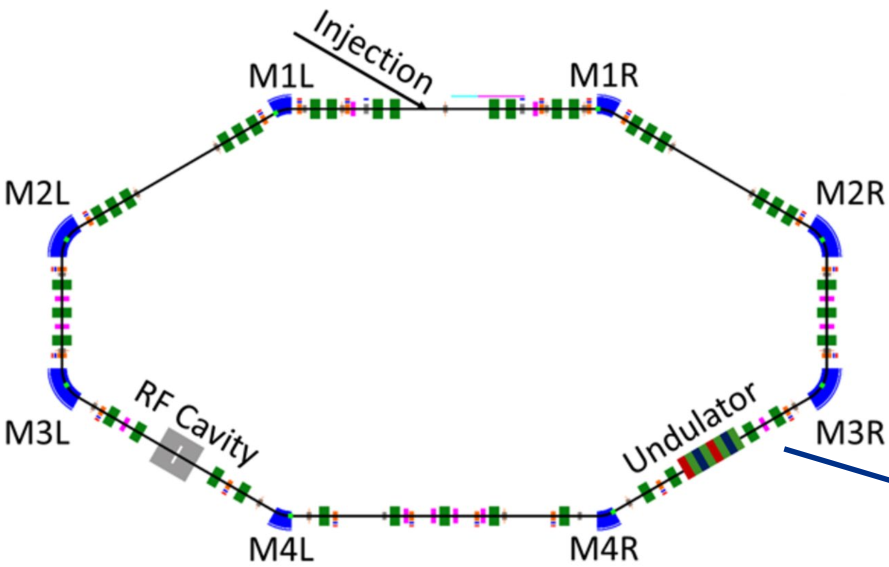

photo credit Evan Angelico

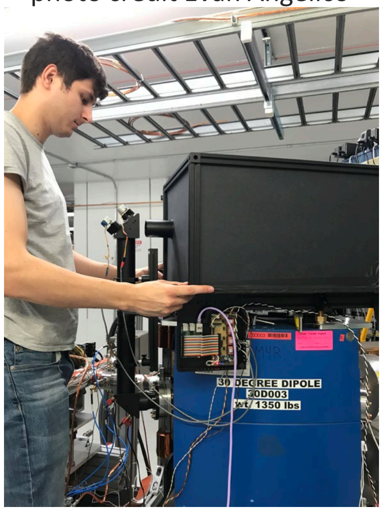

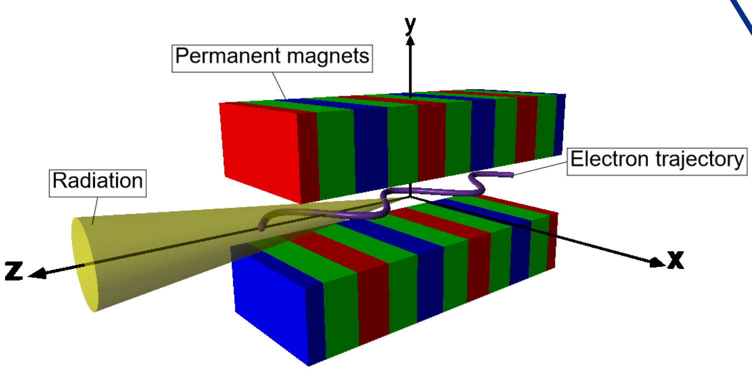

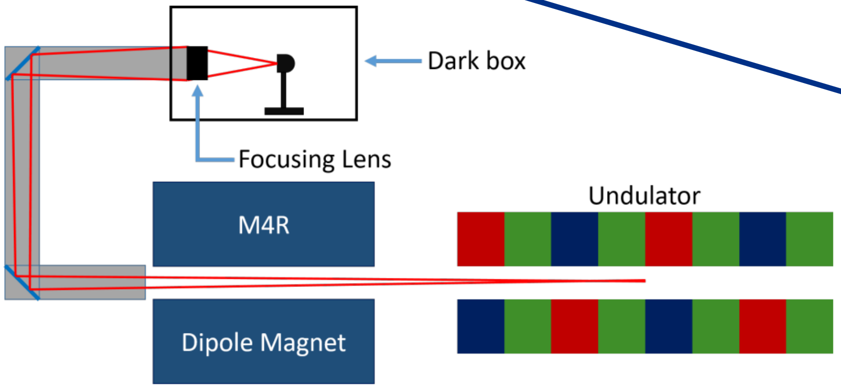

Previous research about statistical properties of synchrotron radiation

Both theoretical and experimental results:

[1] M. C. Teich, T. Tanabe, T. C. Marshall, and J. Galayda, Statistical properties of wiggler and bending-magnet radiation from the Brookhaven Vacuum-Ultraviolet electron storage ring, Phys. Rev. Lett. **65**, 3393 (1990).

[2] V. Sajaev, *Determination of longitudinal bunch profile using spectral fluctuations of incoherent radiation*, Report No ANL/ASD/CP-100935 (Argonne National Laboratory, 2000).

[3] V. Sajaev, Measurement of bunch length using spectral analysis of incoherent radiation fluctuations, in *AIP Conf. Proc.*, Vol. 732 (AIP, 2004) pp. 73–87.

[4] F. Sannibale, G. Stupakov, M. Zolotorev, D. Filippetto, and L. Jägerhofer, Absolute bunch length measurements by incoherent radiation fluctuation analysis, Phys. Rev. ST Accel. Beams **12**, 032801 (2009).

[5] P. Catravas, W. Leemans, J. Wurtele, M. Zolotorev, M. Babzien, I. Ben-Zvi, Z. Segalov, X.-J. Wang, and V. Yakimenko, Measurement of electron-beam bunch length and emittance using shot-noise-driven fluctuations in incoherent radiation, Phys. Rev. Lett. **82**, 5261 (1999).

[6] K.-J. Kim, Start-up noise in 3-D self-amplified spontaneous emission, Nucl. Instrum. Methods Phys. Res., Sect. A **393**, 167 (1997).

[7] S. Benson and J. M. Madey, Shot and quantum noise in free electron lasers, Nucl. Instrum. Methods Phys. Res., Sect. A **237**, 55 (1985).

[8] E. L. Saldin, E. Schneidmiller, and M. V. Yurkov, *The physics of free electron lasers* (Springer Science & Business Media, 2013).

[9] C. Pellegrini, A. Marinelli, and S. Reiche, The physics of x-ray free-electron lasers, Rev. Mod. Phys. **88**, 015006 (2016).

[10] W. Becker and M. S. Zubairy, Photon statistics of a free-electron laser, Phys. Rev. A **25**, 2200 (1982).

[11] W. Becker and J. McIver, Fully quantized many-particle theory of a free-electron laser, Phys. Rev. A **27**, 1030 (1983).

[12] W. Becker and J. McIver, Photon statistics of the free-electron-laser startup, Phys. Rev. A **28**, 1838 (1983).

[13] T. Chen and J. M. Madey, Observation of sub-Poisson fluctuations in the intensity of the seventh coherent spontaneous harmonic emitted by a RF linac free-electron laser, Phys. Rev. Lett. **86**, 5906 (2001).

[14] J.-W. Park, *An Investigation of Possible Non-Standard Photon Statistics in a Free-Electron Laser*, Ph.D. thesis, University of Hawaii at Manoa (2019).

Two experiments to study statistical properties of <u>undulator radiation</u> in IOTA

- Experiment #1 with **many electrons** $(\sim 10^9)$
  - Fundamental harmonic, $\approx 1.1\ \mu\mathrm{m}$
  - InGaAs PIN photodiode
  - Feb-Apr 2019, Feb-Mar 2020

InGaAs PIN photodiode

- Experiment #2 with a **single electron**
  - Second harmonic, $450 - 800\ \mathrm{nm}$
  - Single Photon Avalanche Diode (SPAD)
  - Feb-Mar 2020 + Spring-Summer 2021

Single Photon Avalanche Diode (SPAD)

Turn-by-turn data in both experiments

Experiment #1 --- many electrons ($\sim 10^9$)

Fundamental of the undulator radiation 1.16 um

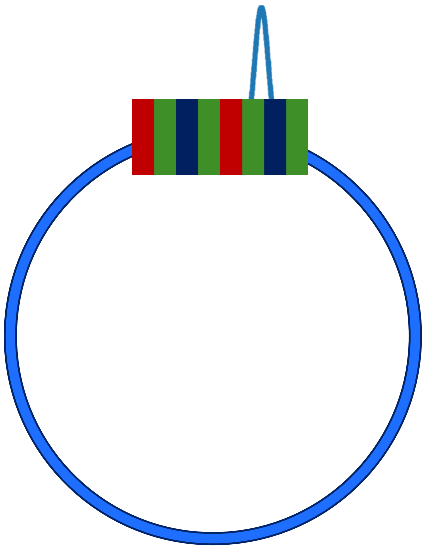

InGaAs PIN photodiode

Revolution number	Number of photocounts, N
0	9994352
1	9997379
2	10002465
3	9999482
4	9996153
...	...
11273 1.5 ms	10000362

$$\mathrm{var}(\mathcal{N}) = \langle \mathcal{N}^2 \rangle - \langle \mathcal{N} \rangle^2$$

Particle loss is negligible during 1.5 ms

Relative fluctuaitons $\sim 10^{-4} - 10^{-3}$ (rms).

The initial goal was to systematically study var($\mathcal{N}$) as a function of the electron bunch parameters (charge, size, shape, divergence)

Then, we realized that we could reverse this procedure and infer the electron bunch parameters from the measured $\mathrm{var}(\mathcal{N})$

Theoretical predictions

$$\mathrm{var}(\mathcal{N}_{\mathrm{ph}}) = \langle \mathcal{N}_{\mathrm{ph}} \rangle + \frac{1}{M} \langle \mathcal{N}_{\mathrm{ph}} \rangle^2$$

Discrete quantum nature of light (Poisson fluctuations)

Turn-to-turn variations in relative electron positions and directions of motion

Page 28:

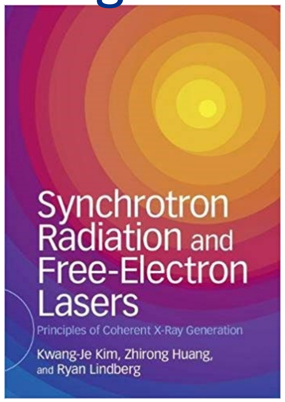

M is conventionally called the number of coherent modes

Simplified 1D model:

Pulses emitted by the electrons:

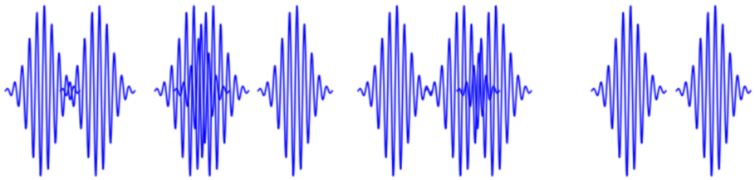

$$W \propto \int \mathrm{d}t \left| \sum_{i=1}^{n_e} E(t - t_i) \right|^2 = \int \mathrm{d}\omega \, |E(\omega)|^2 \left| \sum_{i=1}^{n_e} e^{-i\omega t_i} \right|^2$$

The set of arrival times of the electrons $\{t_i\}$ is different during every revolution in the ring. Hence, the radiated energy W fluctuates from turn to turn. $\sigma_t = \sqrt{\langle t_i^2 \rangle - \langle t_i \rangle^2}$

$$|E(\omega)|^2 \propto e^{-\frac{(\omega - \omega_0)^2}{2\sigma_\omega^2}} \Rightarrow M = \sqrt{1 + 4\sigma_\omega^2 \sigma_t^2}$$

General case

In general, M is a function of

- Detector's angular acceptance
- Detector's spectral sensitivity, polarization sensitivity
- Spectral-angular properties of the radiation (undulator or bending magnet)
- Electron bunch density distribution over x, y, z, $\boxed{x', y', \delta_p}$

We accounted for this part for the first time

Featured in Physics   Open Access

Measurements of undulator radiation power noise and comparison with *ab initio* calculations

Ihar Lobach, Sergei Nagaitsev, Valeri Lebedev, Aleksandr Romanov, Giulio Stancari, Alexander Valishev, Aliaksei Halavanau, Zhirong Huang, and Kwang-Je Kim

Phys. Rev. Accel. Beams **24**, 040701 – Published 1 April 2021

Physics See synopsis: Using Fluctuations to Measure Beam Properties

32

More

Fermilab

The obtained expression is very complex and includes a multidimensional integral:

$$\boxed{\frac{1}{M} = (1 - 1/n_e)\frac{\sqrt{\pi}}{\sigma_z^{\mathrm{eff}}}\frac{\int \mathrm{d}k\mathrm{d}^2\boldsymbol{\phi}_1\mathrm{d}^2\boldsymbol{\phi}_2\mathrm{d}^2\boldsymbol{r}'\mathcal{P}_k(\boldsymbol{r}',\boldsymbol{\phi}_1-\boldsymbol{\phi}_2)\mathcal{I}_k(\boldsymbol{\phi}_1,\boldsymbol{r}')\mathcal{I}_k^*(\boldsymbol{\phi}_2,\boldsymbol{r}')}{\langle\mathcal{N}_{\mathrm{s.e.}}\rangle^2},} \quad (2)$$

with

$$\mathcal{P}_k(\boldsymbol{r}',\boldsymbol{\phi}_1-\boldsymbol{\phi}_2) = \frac{1}{4\pi\sigma_{x'}\sigma_{y'}} e^{-\frac{(x')^2}{4\sigma_{x'}^2}-\frac{(y')^2}{4\sigma_{y'}^2}} e^{-ik\Delta_x(\phi_{1x}-\phi_{2x})x'-ik\Delta_y(\phi_{1y}-\phi_{2y})y'} e^{-k^2\Sigma_x^2(\phi_{1x}-\phi_{2x})^2-k^2\Sigma_y^2(\phi_{1y}-\phi_{2y})^2}, \quad (3)$$

$$\mathcal{I}_k(\boldsymbol{\phi},\boldsymbol{r}') = \sum_{s=1,2}\eta_{k,s}(\boldsymbol{\phi})\mathcal{E}_{k,s}(\boldsymbol{\phi})\mathcal{E}_{k,s}^*(\boldsymbol{\phi}-\boldsymbol{r}'), \quad (4)$$

$$\langle\mathcal{N}_{\mathrm{s.e.}}\rangle = \sum_{s=1,2}\int \mathrm{d}k\mathrm{d}^2\boldsymbol{\phi}\,\eta_{k,s}(\boldsymbol{\phi})|\mathcal{E}_{k,s}(\boldsymbol{\phi})|^2, \quad (5)$$

where $s = 1, 2$ indicates the polarization component, n_e is the number of electrons in the bunch, $k = 2\pi/\lambda$ is the magnitude of the wave vector; $\boldsymbol{\phi} = (\phi_x, \phi_y)$, $\boldsymbol{\phi}_1 = (\phi_{1x}, \phi_{1y})$ and $\boldsymbol{\phi}_2 = (\phi_{2x}, \phi_{2y})$ represent angles of direction of the radiation in the paraxial approximation. Hereinafter, x and y refer to the horizontal and the vertical axes, respectively, and

$$\boxed{\sigma_z^{\mathrm{eff}} = 1\Big/\left(2\sqrt{\pi}\int\rho^2(z)\mathrm{d}z\right)} \quad (6)$$

where $\rho(z)$ is the electron bunch longitudinal density distribution function, $\int\rho(z)\mathrm{d}z = 1$, and σ_z^{eff} is equal to the rms bunch length σ_z for a Gaussian bunch; $\boldsymbol{r}' = (x', y')$ represents the direction of motion of an electron at the radiator center, relative to a reference electron; $\sigma_{x'}$ and $\sigma_{y'}$ are the rms beam divergences, $\sigma_{x'}^2 = \gamma_x\epsilon_x + D_{x'}^2\sigma_p^2$, $\sigma_{y'}^2 = \gamma_y\epsilon_y$; $\Sigma_x^2 = \epsilon_x/\gamma_x + (\gamma_x D_x + D_{x'}\alpha_x)^2\beta_x\epsilon_x\sigma_p^2/\sigma_{x'}^2$, $\Sigma_y^2 = \epsilon_y/\gamma_y$, $\Delta_x = (\alpha_x\epsilon_x - D_x D_{x'}\sigma_p^2)/\sigma_{x'}^2$, $\Delta_y = \alpha_y/\epsilon_y$, where α_x, β_x, γ_x, α_y, β_y, γ_y are the Twiss parameters of an uncoupled focusing optics in the synchrotron radiation

$$\mathcal{E}_{k,s}(\boldsymbol{\phi}) = \sqrt{\frac{\alpha k}{2(2\pi)^3}}\int \mathrm{d}t\boldsymbol{e}_s(\boldsymbol{k})\cdot\boldsymbol{v}(t)e^{ickt-i\boldsymbol{k}\cdot\boldsymbol{r}(t)}$$

- Transversely Gaussian beam
- Arbitrary longitudinal density distribution

- Assumes known Twiss-functions

The code for numerical computation is available at https://github.com/IharLobach/fur

Quantum optics description

$$\mathrm{var}(\mathcal{N}_{\mathrm{ph}}) = \langle\mathcal{N}_{\mathrm{ph}}\rangle + \frac{1}{M}\langle\mathcal{N}_{\mathrm{ph}}\rangle^2$$

Quantum

Classical

At negligible electron recoil the radiated field is in a **coherent state**:

PHYSICAL REVIEW VOLUME 131, NUMBER 6 15 SEPTEMBER 1963

Coherent and Incoherent States of the Radiation Field*

Roy J. Glauber

$$\boxed{|\alpha\rangle = e^{-\frac{1}{2}|\alpha|^2}\sum_n \frac{\alpha^n}{\sqrt{n!}}|n\rangle}$$

$$\boxed{\mathrm{var}(n) = \langle\alpha|\left(\hat{a}^\dagger\hat{a} - \langle n\rangle\right)^2|\alpha\rangle = |\alpha|^2 = \langle n\rangle}$$

A unified description leading to the above expression is possible withing the framework of **quantum optics using the density operator formalism**:

Open Access

Statistical properties of spontaneous synchrotron radiation with arbitrary degree of coherence

Ihar Lobach, Valeri Lebedev, Sergei Nagaitsev, Aleksandr Romanov, Giulio Stancari, Alexander Valishev, Aliaksei Halavanau, Zhirong Huang, and Kwang-Je Kim

Phys. Rev. Accel. Beams **23**, 090703 – Published 11 September 2020

Details about Experiment #1 --- many electrons (10^9)
Spectral-angular radiation distribution

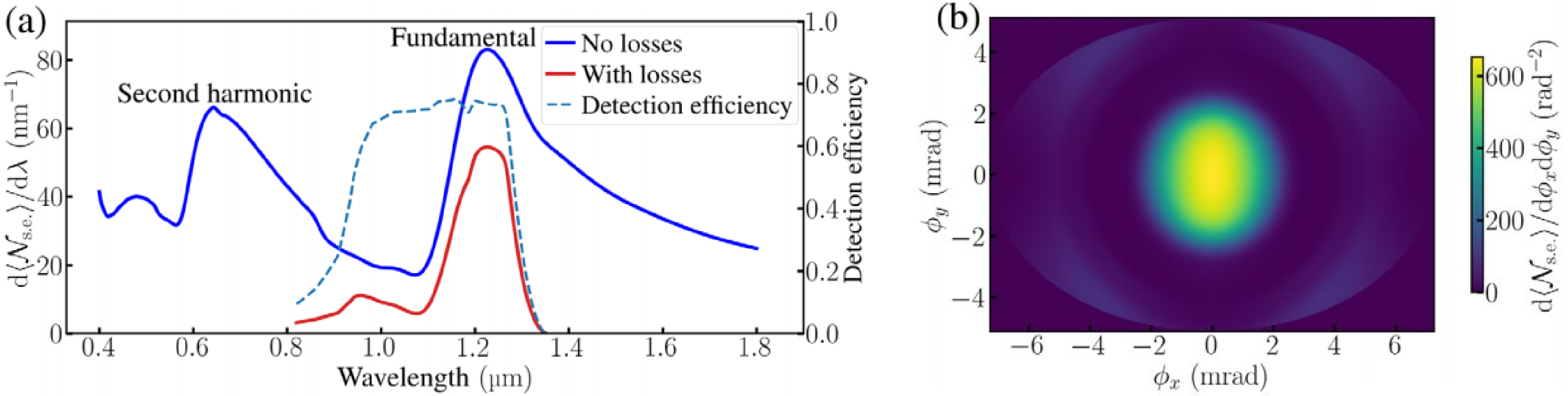

In Experiment #1:

#1 Detect the fundamental (≈ 1.16 um). InGaAs p-i-n photodiode

#2 Wide band (≈ 0.14 um FWHM). Large acceptance angle $> 1/\gamma$

(We use a focusing lens)

Simulated total intensity: 9.1×10^{-3} photoelectrons/electron

Measured: 8.8×10^{-3} photoelectrons/electron

Details about the apparatus

InGaAs PIN photodiode

G11193-10R

Sensitive area: Ø1mm
Quantum efficiency at 1.16 µm: 80%

*the circuit was built by Greg Saewert

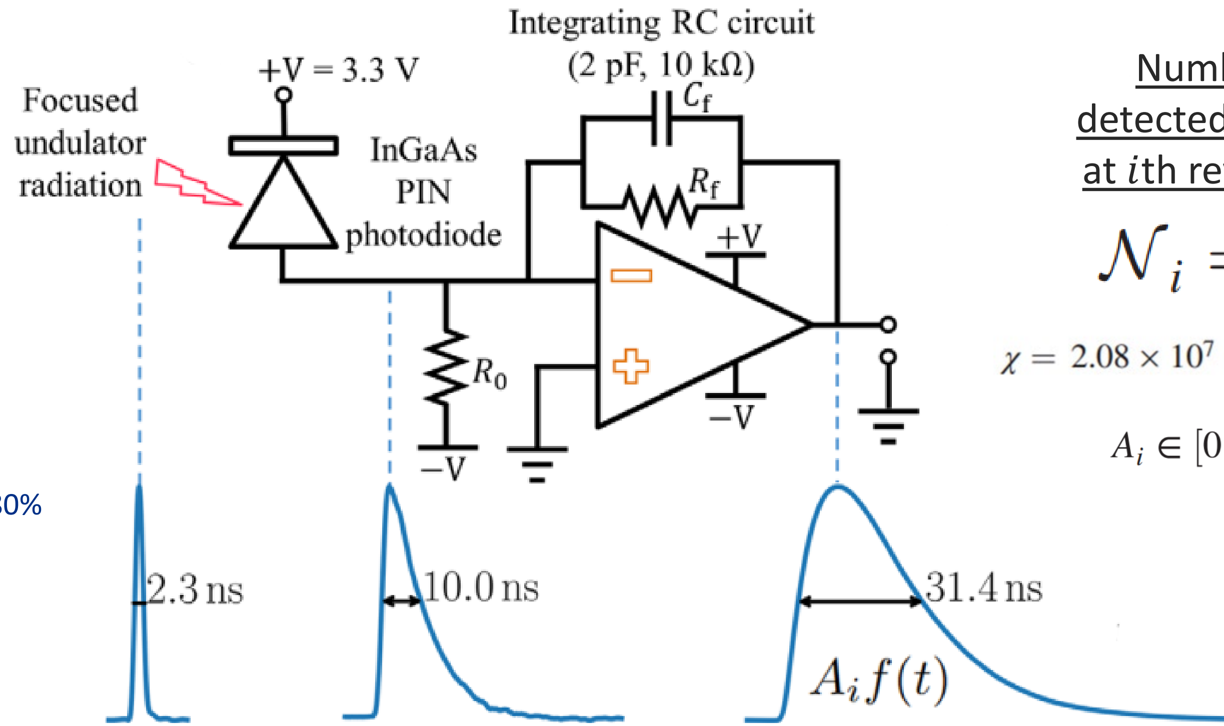

Number of detected photons at ith revolution:

$$\mathcal{N}_i = \chi A_i$$

$\chi = 2.08 \times 10^7$ photoelectrons/V

$A_i \in [0, 1.2]$ V

*Many thanks to Mark Obrycki, Peter Prieto, David Johnson, Todd Johnson and Greg Saewert for the equipment for the setup and for their help during our detector tests.

The expected relative fluctuation of A_i was very small $10^{-4} - 10^{-3}$ (rms).
It was a big challenge to measure it.

*comparable to the resolution of our 8-bit scope

Comb (notch) filter

*the idea to use the comb filter was proposed by S. Nagaitsev.
The components were provided by B.J. Fellenz, K. Carlson, and D. Frolov

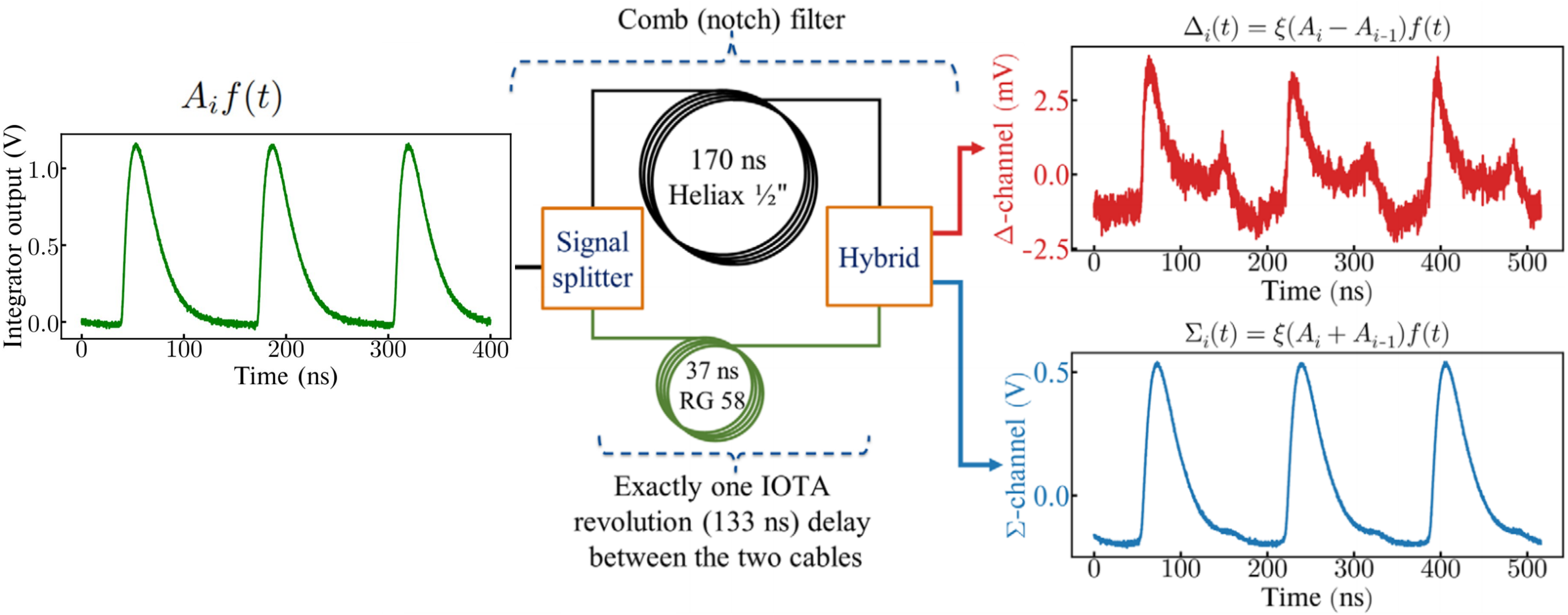

Our comb filter had some imperfections:

- Cross-talk (< 1%)
- Small reflected pulse in one of the arms

*they could be taken into account and did not affect final results

Noise filtering algorithm

- The instrumental noise due to the oscilloscope’s pre-amp and due to the integrator’s op-amp was about 0.3 mV (rms)
- Therefore, signal-to-noise ratio was about 1

We had to use a special noise filtering algorithm.
For each time t within one IOTA revolution, calculate variance of Δ-signal for the 11000 revolutions:

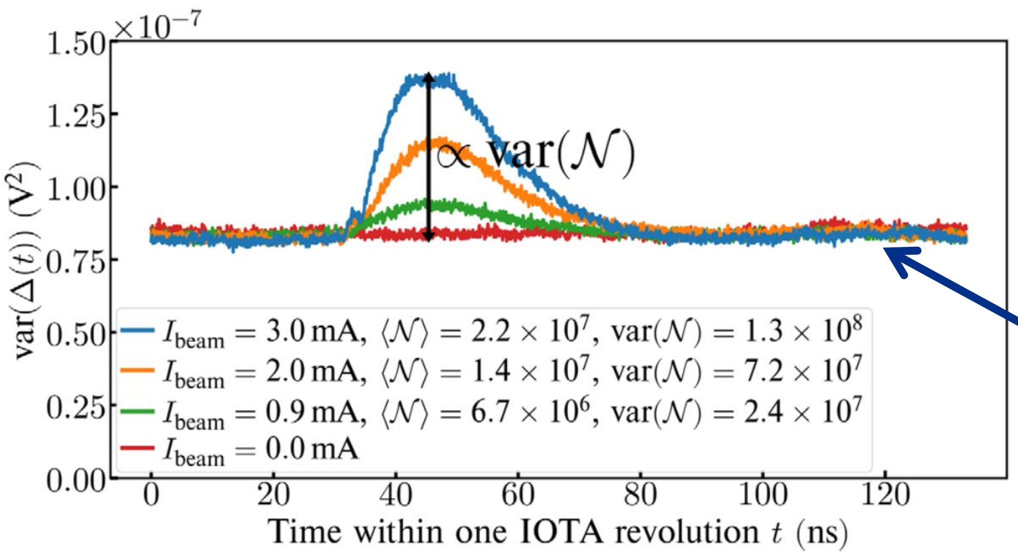

$$\mathrm{var}(\Delta(t)) = 2\xi^2 \mathrm{var}(A) f^2(t) + \mathrm{var}(\nu_\Delta(t))$$

$$\mathrm{var}(\nu_\Delta(t)) = \mathrm{var}(\nu_\Delta) = 8.8 \times 10^{-8}\ \mathrm{V}^2$$

constant noise level

Measurements and simulations

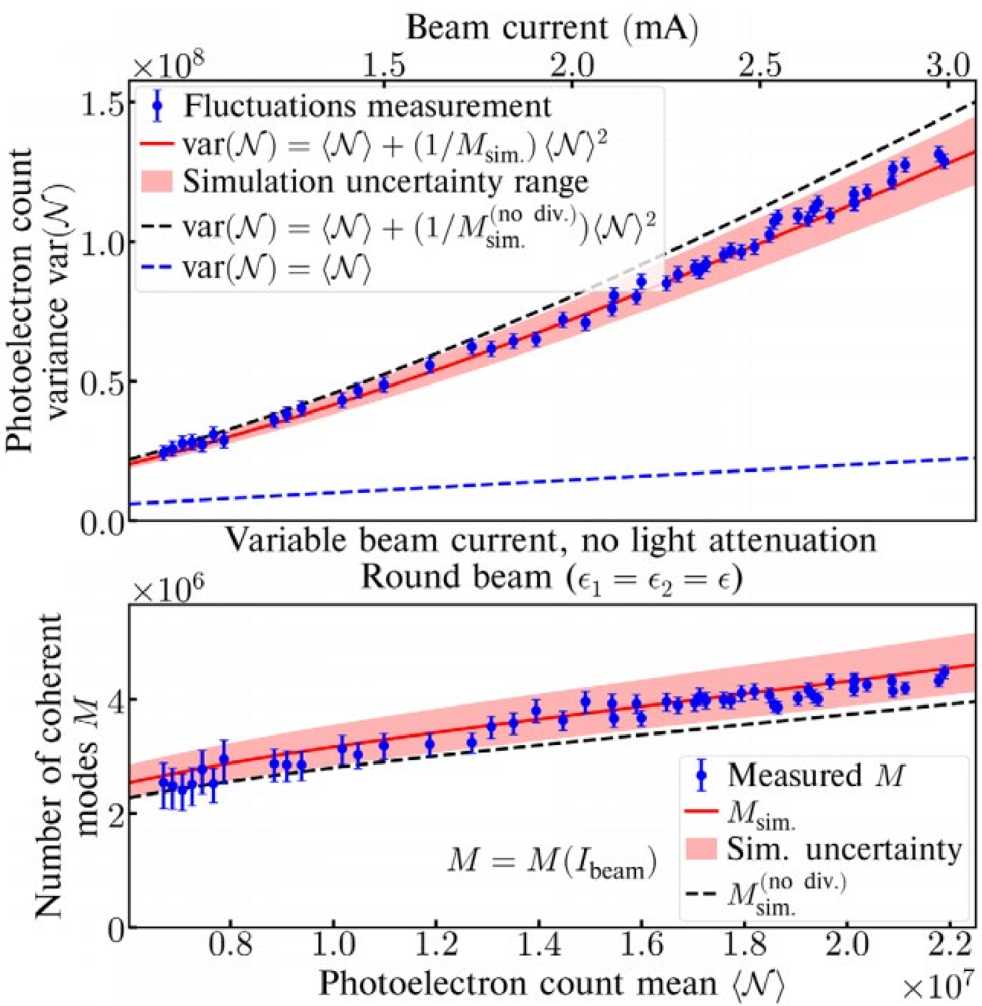

$$M = M(\epsilon_x, \epsilon_y, \sigma_p, \sigma_z^{\mathrm{eff}})$$

For the simulation,

- ϵ_x and ϵ_y were estimated using bending magnet synchrotron radiation monitors and known Twiss functions.
- σ_z^{eff} and σ_p were estimated using the wall-current monitor signal

Note that the simulation with beam divergence taken into account agrees better

Measurement of transverse bunch size: 7 synclight stations

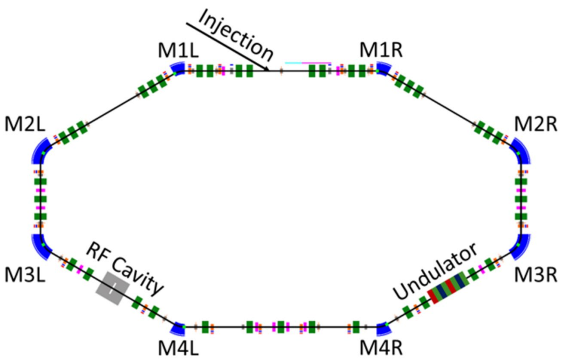

Bending magnet radiation (not undulator)

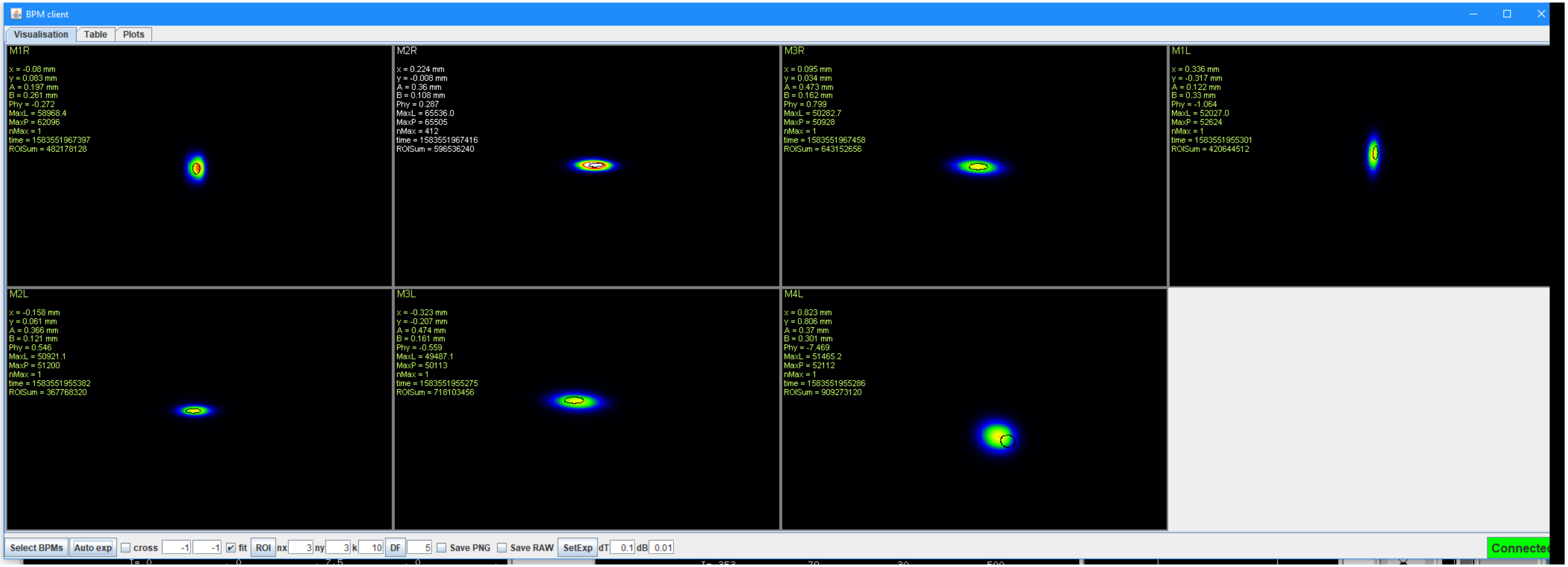

*built by A. Romanov, J. Santucci, G. Stancari, N. Kuklev, …

Measurement of longitudinal bunch length and shape: Bunch length monitor

- Wall-current monitor → long cable → amplifier → oscilloscope
- The web-server runs on a Raspberry Pi on the Fermilab controls network. It receives the signal from the scope and applies the inverse of the transmission function of the long cable and the amplifier to reconstruct the shape of the electron bunch

$\sigma_z = 20 - 30$ cm

$\sigma_p \approx 9.1 \times 10^{-6} \times \sigma_z[\text{cm}]$

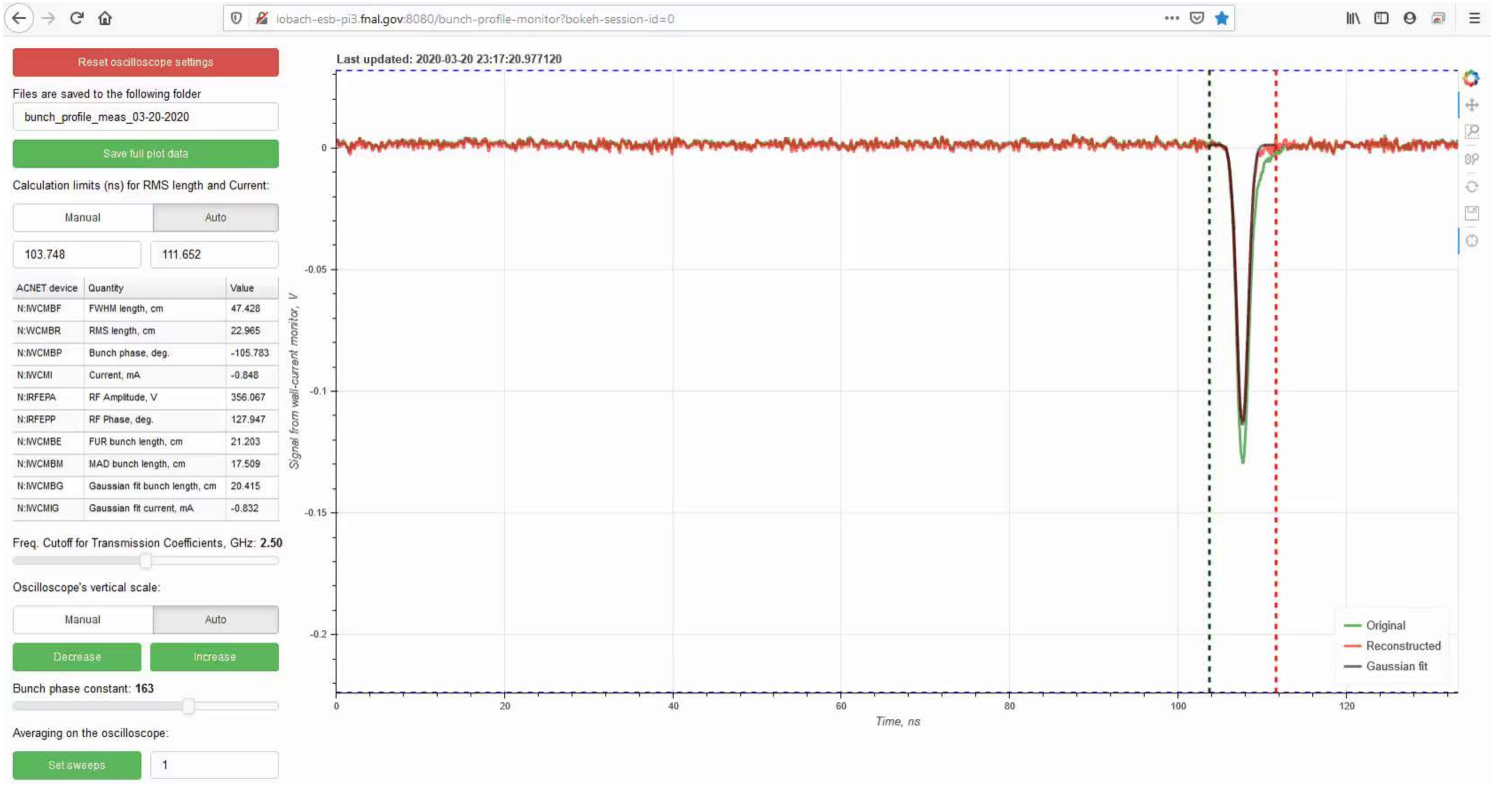

Valeri Lebedev and Kermit Carlson helped with measurement of the transmission function.
Dean Edstrom helped with network communication with the oscilloscope.

Fermilab

Neutral density (ND) filters

- ND filter is a filter that has constant attenuation in a wide spectral range
- ND filter does not change the number of coherent modes M, however, it does change the average number of detected photons $\langle \mathcal{N} \rangle$

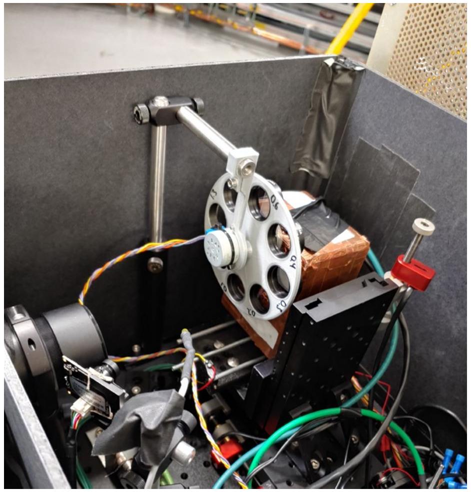

The filter wheel was built by Sasha Romanov

Remote controls for the apparatus

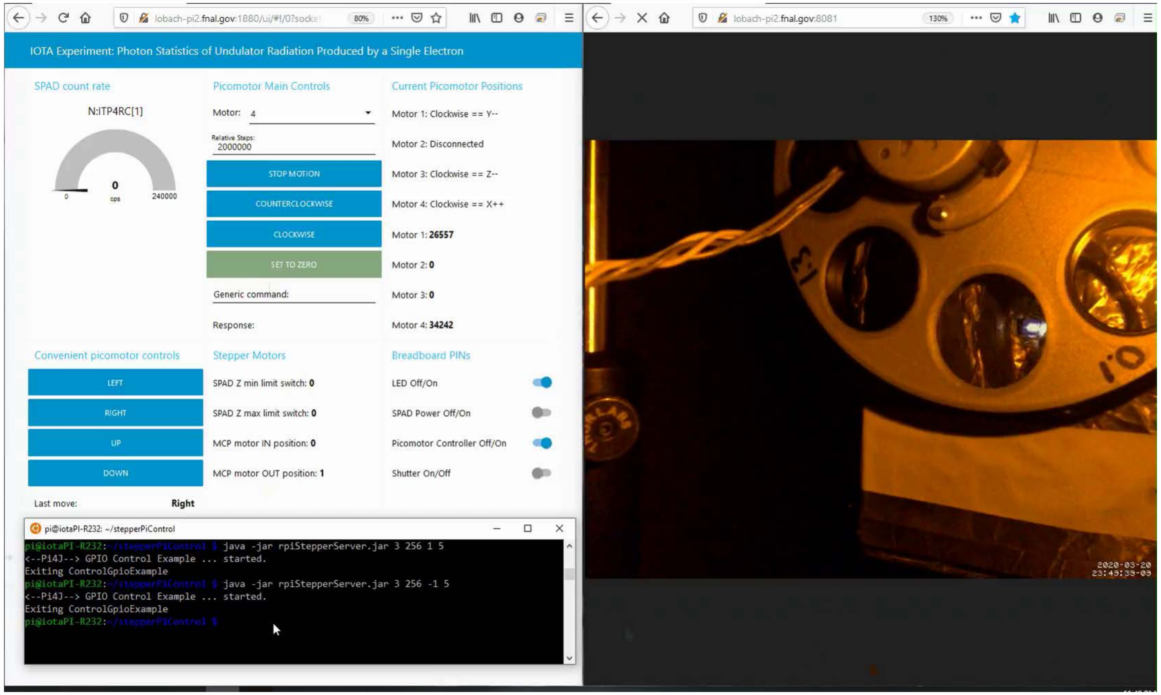

Measurements with ND filters (right-hand side)

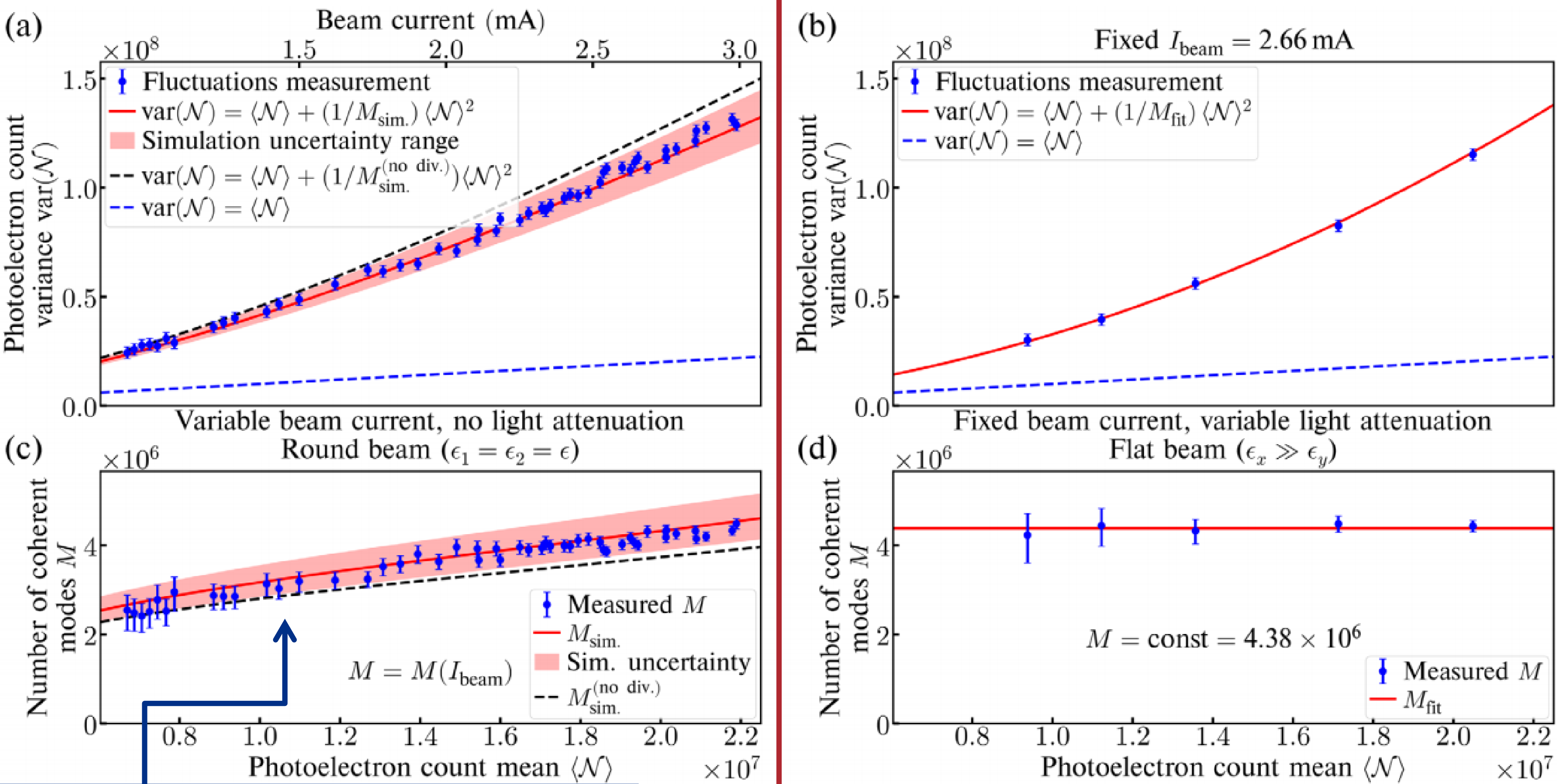

ϵ_x, ϵ_y, σ_z^{eff}, σ_p change with the beam current due to intrabeam scattering and interaction of the bunch with its environment. Therefore, M changes too.

Reconstruction of transverse emittances from the measured $\mathrm{var}(\mathcal{N})$

Featured in Physics Editors' Suggestion Open Access

Transverse Beam Emittance Measurement by Undulator Radiation Power Noise

Ihar Lobach, Sergei Nagaitsev, Valeri Lebedev, Aleksandr Romanov, Giulio Stancari, Alexander Valishev, Aliaksei Halavanau, Zhirong Huang, and Kwang-Je Kim
Phys. Rev. Lett. **126**, 134802 – Published 1 April 2021

Physics See synopsis: Using Fluctuations to Measure Beam Properties

We verified our method with a “round” beam, whose emittances could be independently measured by synchrotron radiation monitors, (a) and (c):

Then, we used our fluctuations-based method to **measure the unknown small vertical emittance of a “flat” beam**, (b) and (d):

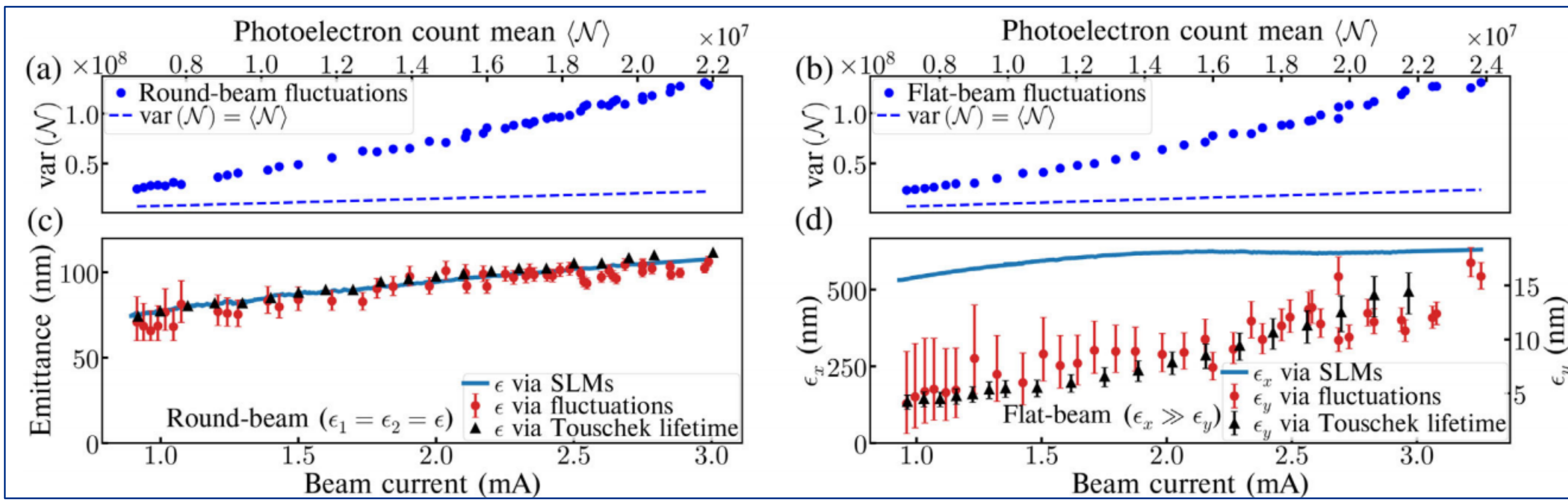

Strong coupling

Uncoupled

Limitations (or strengths?)

- The fluctuations must not be dominated by the Poisson noise

$$\langle\mathcal{N}\rangle \lesssim \frac{1}{M}\langle\mathcal{N}\rangle^2 \Rightarrow \frac{\langle\mathcal{N}\rangle}{M} = \alpha\left(\frac{\pi}{2}\right)^{\frac{3}{2}} F_h(K_\mathrm{u})\frac{\gamma^2 N_\mathrm{u}^2 n_e}{\sigma_x\sigma_y\sigma_z k_0^3} \gtrsim 1$$

- M must be sensitive to changes in σ_x, σ_y (ϵ_x, ϵ_y)

$$\sigma_x, \sigma_y \gtrsim \sqrt{2L_\mathrm{u}\lambda_0}/(4\pi)$$

The sensitivity of this technique improves with shorter wavelength. Therefore, this technique may be particularly beneficial for existing state-of-the-art and next-generation low-emittance high-brightness ultraviolet and x-ray synchrotron light sources. For instance, this technique can measure $\epsilon_x \approx \epsilon_y \approx 30$ pm in the Advanced Photon Source Upgrade at Argonne.

Usage of slits and masks

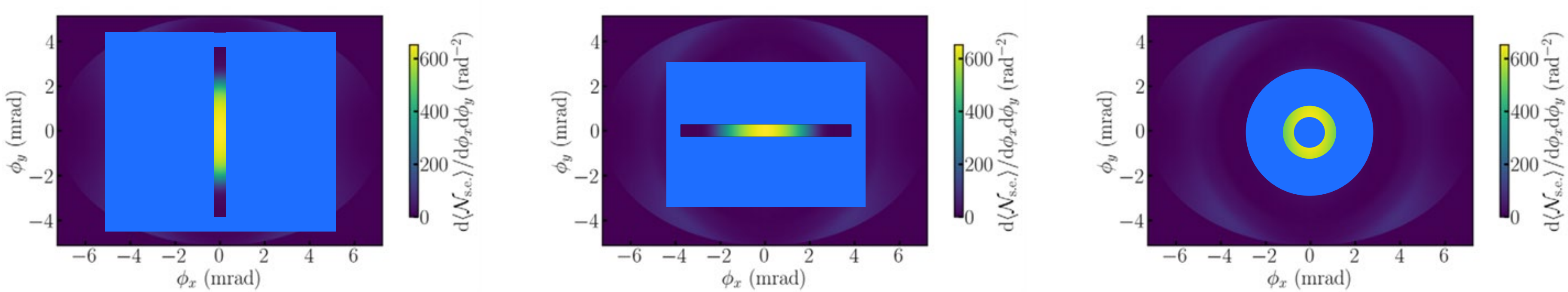

- Measurement of fluctuations with slits or masks would allow measurement of more than one electron bunch parameter.

Original angular distribution:

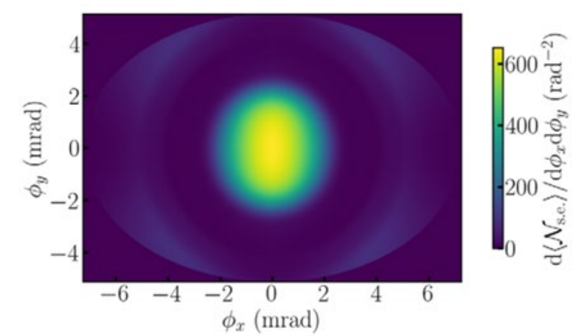

$$M = \sqrt{1+4\sigma_k^2\sigma_z^2}\sqrt{1+4k_0^2\sigma_{\theta_x}^2\sigma_x^2}\sqrt{1+4k_0^2\sigma_{\theta_y}^2\sigma_y^2}$$

Fermilab

Experiment #2 --- a single electron in the ring

Next step is a single electron because it is free from any collective effects. It is a very repeatable and well controlled system to study possible deviations from Poisson statistics.

Goal #1 Verify that the photostatistics in the single-electron case is Poissonian:

$$\mathrm{var}(\mathcal{N}) = \langle\mathcal{N}\rangle + \cancel{\frac{1}{M}\langle\mathcal{N}\rangle^2}$$

Super-Poissonian light:

$$\mathrm{var}(\mathcal{N}) > \langle\mathcal{N}\rangle$$

Sub-Poissonian light:

$$\mathrm{var}(\mathcal{N}) < \langle\mathcal{N}\rangle$$

unusual – non-classical state of the radiated field

Most sources suggest Poissonian photostatistics for a single electron (at negligible electron recoil):

PHYSICAL REVIEW VOLUME 131, NUMBER 6 15 SEPTEMBER 1963

Coherent and Incoherent States of the Radiation Field*

Roy J. Glauber

Lyman Laboratory of Physics, Harvard University, Cambridge, Massachusetts

(Received 29 April 1963)

However, this fairly similar experiment reports observation of Sub-Poissonian statistics:

VOLUME 86, NUMBER 26 PHYSICAL REVIEW LETTERS 25 JUNE 2001

Observation of Sub-Poisson Fluctuations in the Intensity of the Seventh Coherent Spontaneous Harmonic Emitted by a rf Linac Free-Electron Laser

Teng Chen and John M. J. Madey

Department of Physics and Astronomy, University of Hawaii at Manoa, Honolulu, Hawaii 96822

(Received 18 April 2000)

Goal #2 Use the photocount arrival time information to study the synchrotron motion of the single electron

Obtaining a single electron in the ring

- Injecting very low current from linac
- Changing RF voltage quickly to scrape electrons
- The number of electrons is easily determined by looking at photocounts rate
- Lifetime ≈1-2 hours

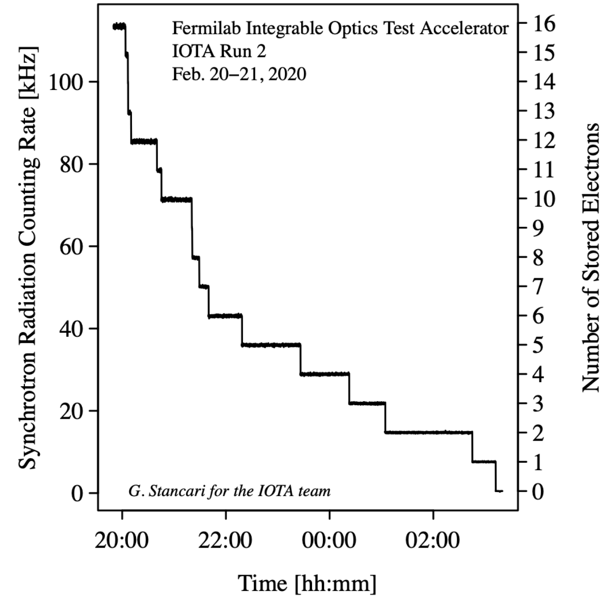

- Real time footage of **one electron** from M2R camera after specially developed noise cancellation algorithms (bending magnet radiation)
  - Clearly visible “stopping” points are due to integration time of less than damping time

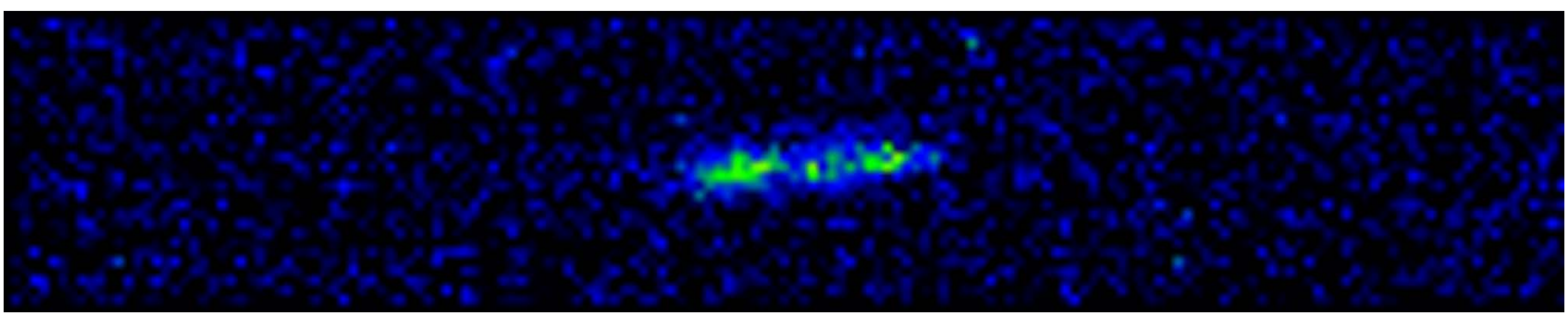

*video borrowed from Sasha Romanov’s presentation at the workshop “Single-electron experiments in IOTA”

Design of the experiment with a single electron

Picosecond event timer
(provided by Giulio Stancari)

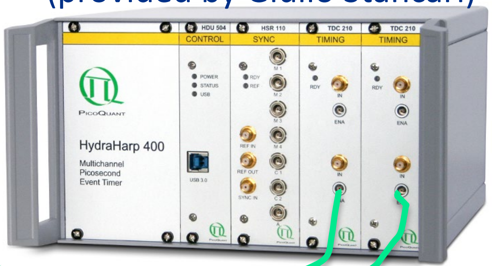

IOTA revolution marker

Record all events for 20 sec – 2 min

	Revolution number	Detection time relative to IOTA revolution marker, ps
0	51	62977.0
1	171	64337.0
2	239	62389.0
3	598	63454.0
4	999	64303.0
...	...	...
1490071	450123392	63592.0
1490072	450123677	62846.0
1490073	450123880	62373.0
1490074	450123931	62842.0
1490075	450124364	62746.0

1490076 rows × 2 columns

*on average one detection per 304 revolutions

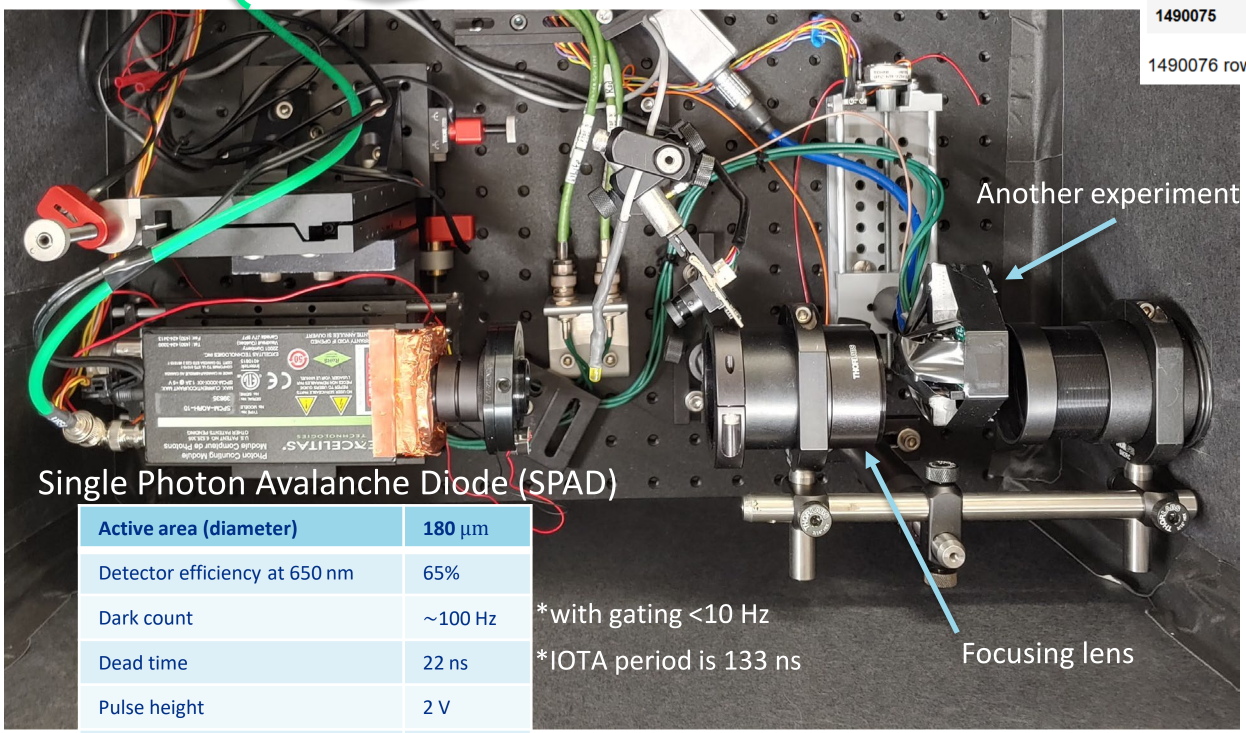

Active area (diameter)	180 μm
Detector efficiency at 650 nm	65%
Dark count	~100 Hz
Dead time	22 ns
Pulse height	2 V
Pulse length	10 ns

Undulator radiation

*the stepper motor translation stages were provided by Sasha Romanov

Controls

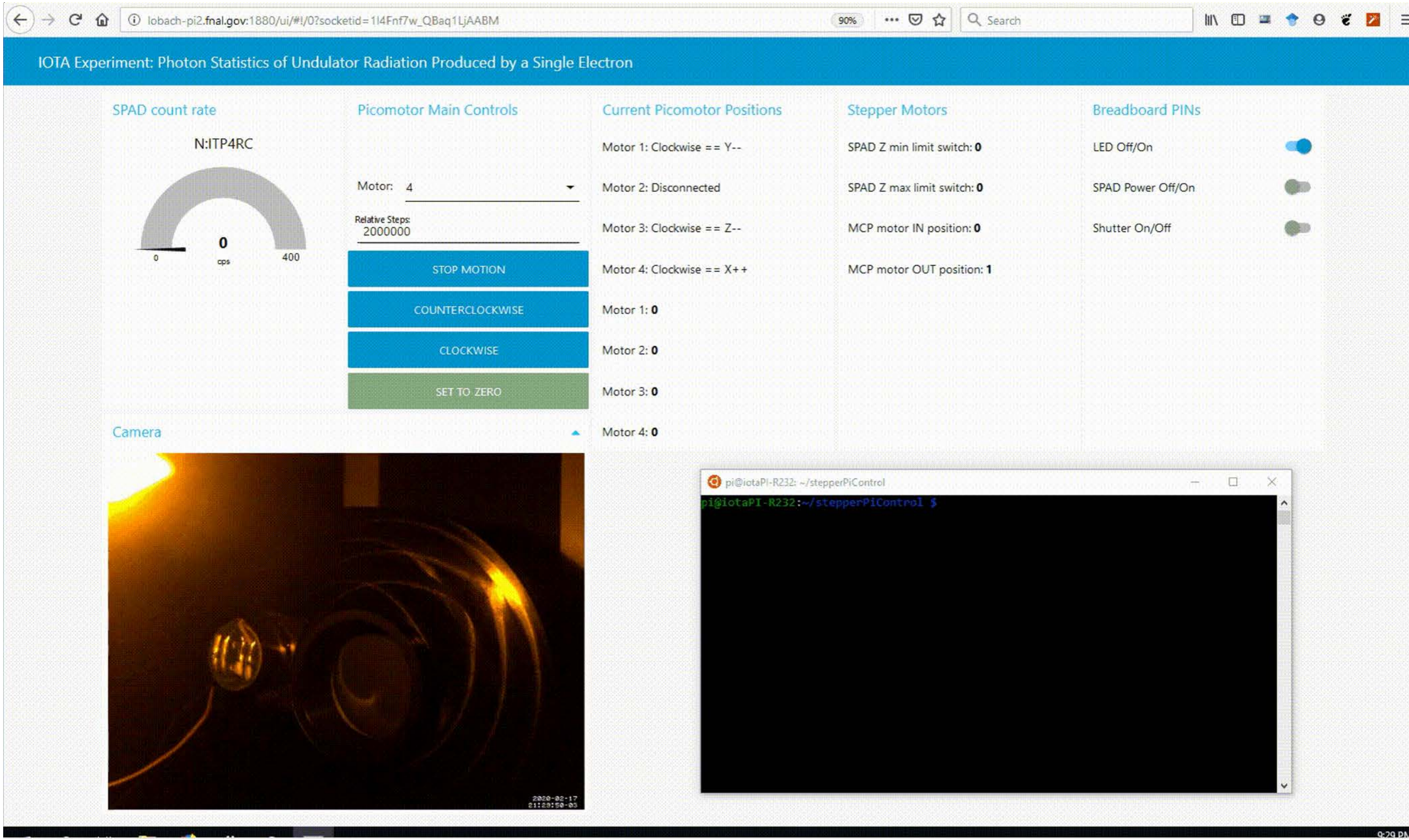

- Live camera video
- x, y, z motors
- Photocount rate
- Optical shutter
- Detector power switch
- LED power switch

Photocount rate. Simulation vs. measurements

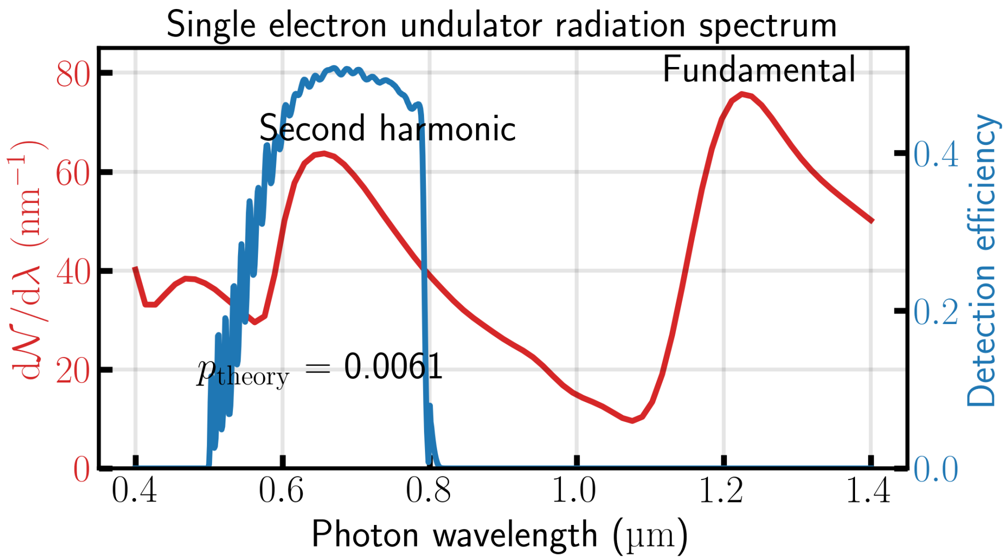

Total efficiency in the simulation takes into account:

- two mirrors
- vacuum chamber window
- one lens
- low-pass filter
- high-pass filter
- quantum efficiency of the detector.

Simulated photocount rate for one electron (assuming focusing to a point): 46kHz

However, aberrations in the lens and the diffraction limit result in a nonzero light spot size in the focal plane and not all the light is collected by the detector:

*dark counts: ≈ 100Hz (with gating ≈ 4Hz)

Measured rate for one electron: 25kHz, i.e., 1 detection per 304 IOTA revolutions

Angular intensity distribution

Simulation:

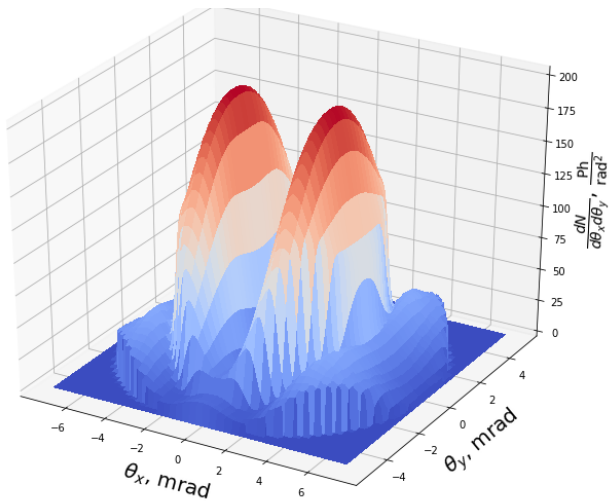

Photo:

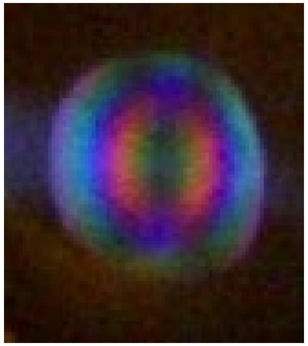

7 measured x-scans at different values of y (far from the focal plane):

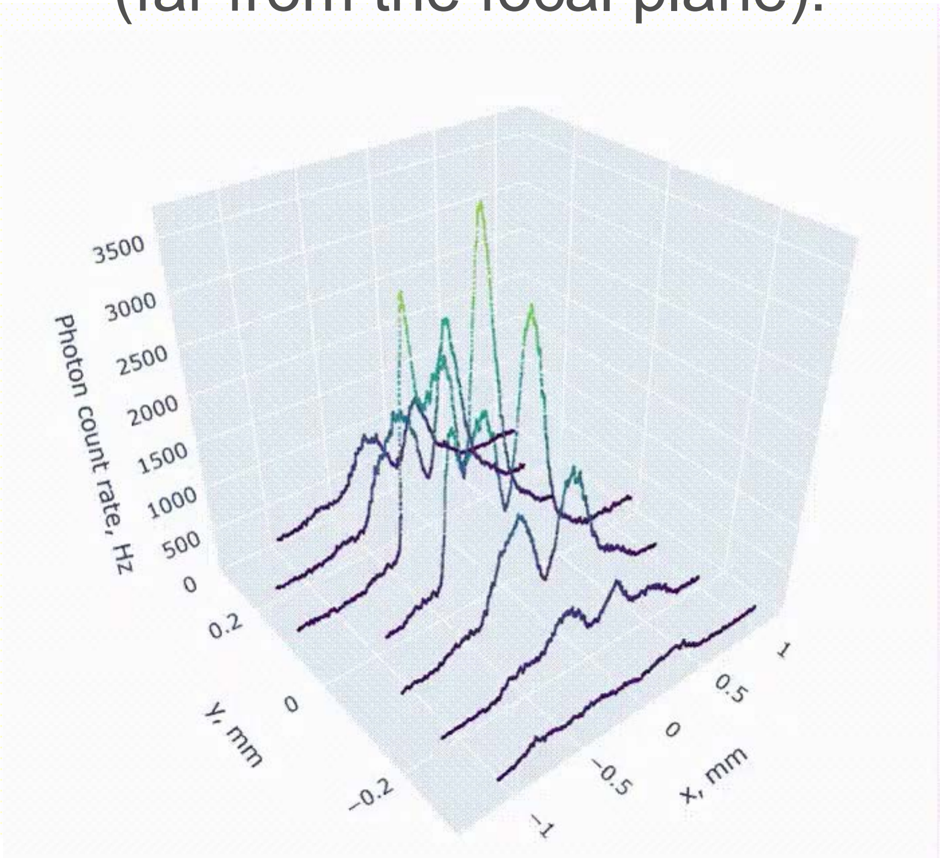

Analysis of the statistical properties

*on average one detection per 304 revolutions
*Probability to detect a photon(s) in one revolution: $p = 0.00330$

Collected data (binary detector):

000001000000110000000000001000100000000111000000000…

0 - no detection, 1 – one or more photons detected

~~Poisson distribution~~ → **Bernoulli trials**: $\mathrm{var}(\mathcal{N}) = (1-p)\langle\mathcal{N}\rangle$

Distribution of interarrival times: geometric

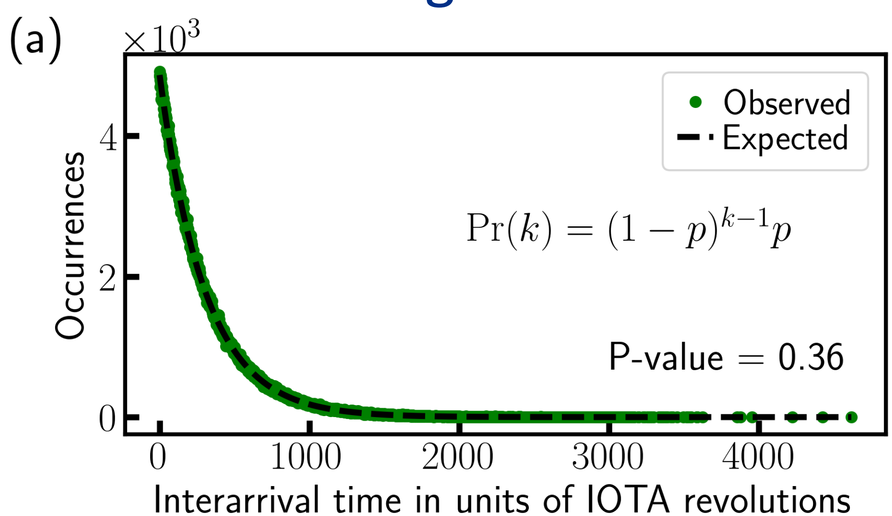

Distribution of photocounts in a time window: binomial

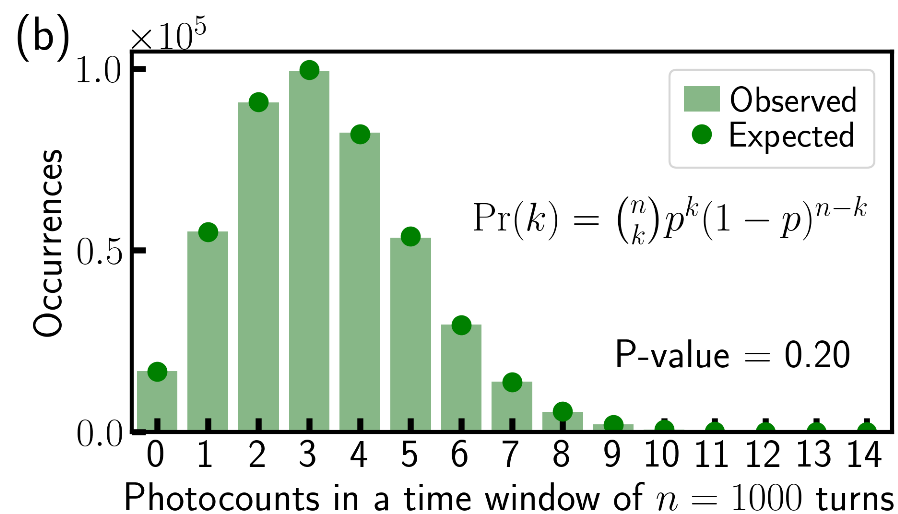

P-value – for hypotheses testing (χ^2 goodness of fit test)

Measurements with two SPAD detectors

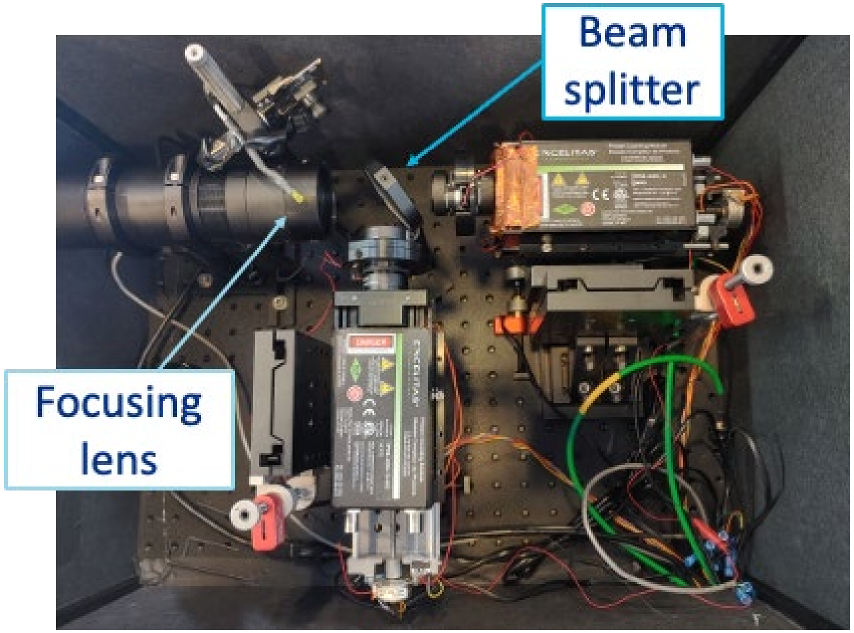

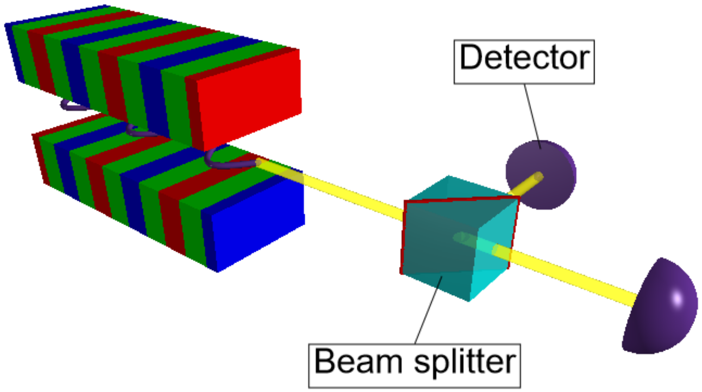

Collected data:

00000100000110000000000200010000000112000000...

- So far, no deviations from our expectations

Detector #1: ~30 kHz

Detector #2: ~15 kHz

Detector #1 & Detector #2: ~70 Hz

No correlation or anticorrelation between the two detectors

Future experiments: Mach-Zehnder interferometry

- Interference of the photons in emitted photon pairs with two detectors:

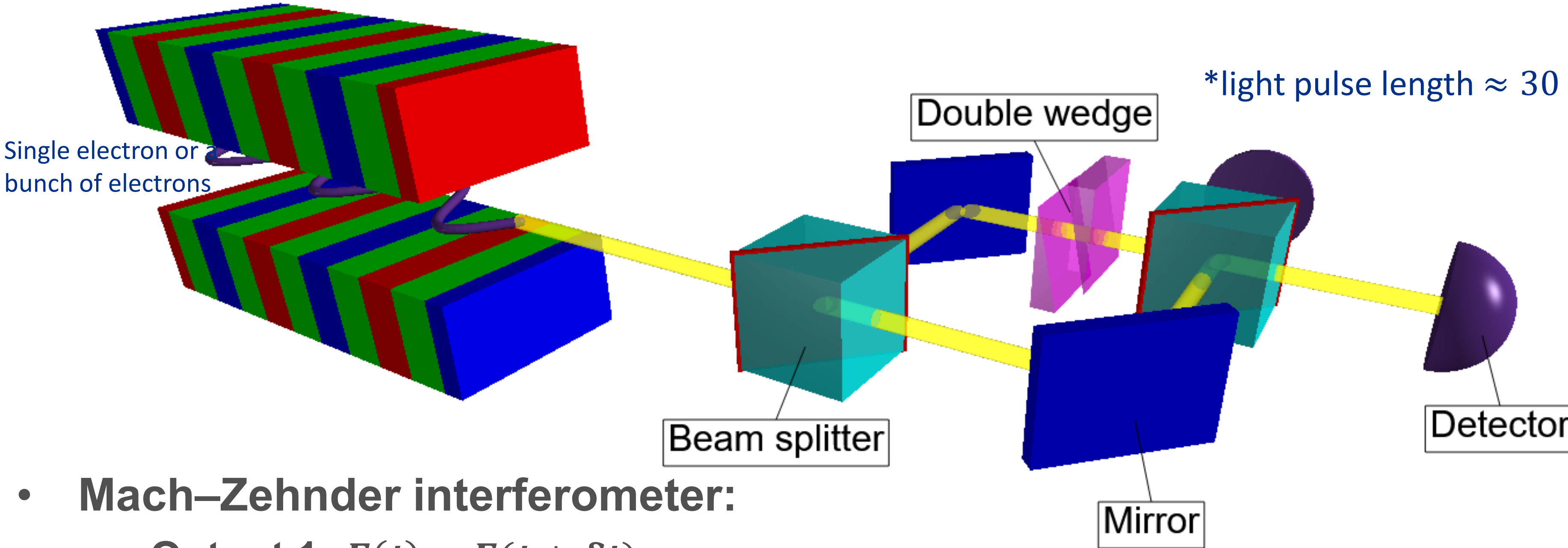

*light pulse length ≈ 30 fs

- **Mach–Zehnder interferometer:**
  - **Output 1:** $E(t) - E(t + \delta t)$
  - **Output 2:** $E(t) + E(t + \delta t)$

In some sense, this is a measurement of the light pulse shape in time domain

This experiment is currently under preparation by Alexander Shemyakin, Aleksandr Romanov, Sergei Nagaitsev, Jonathan Jarvis, and Giulio Stancari

MZ fringes with a HeNe laser (test light source)

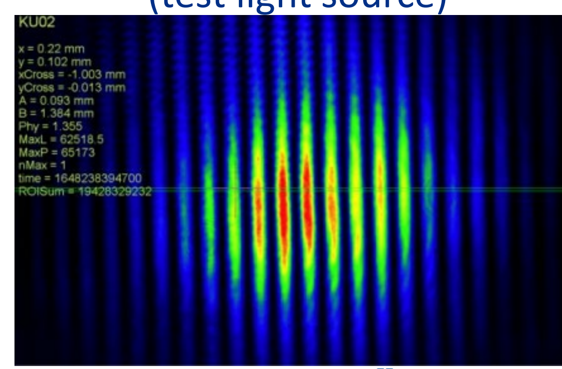

A possible diagnostic tool: Synchrotron motion of a single electron

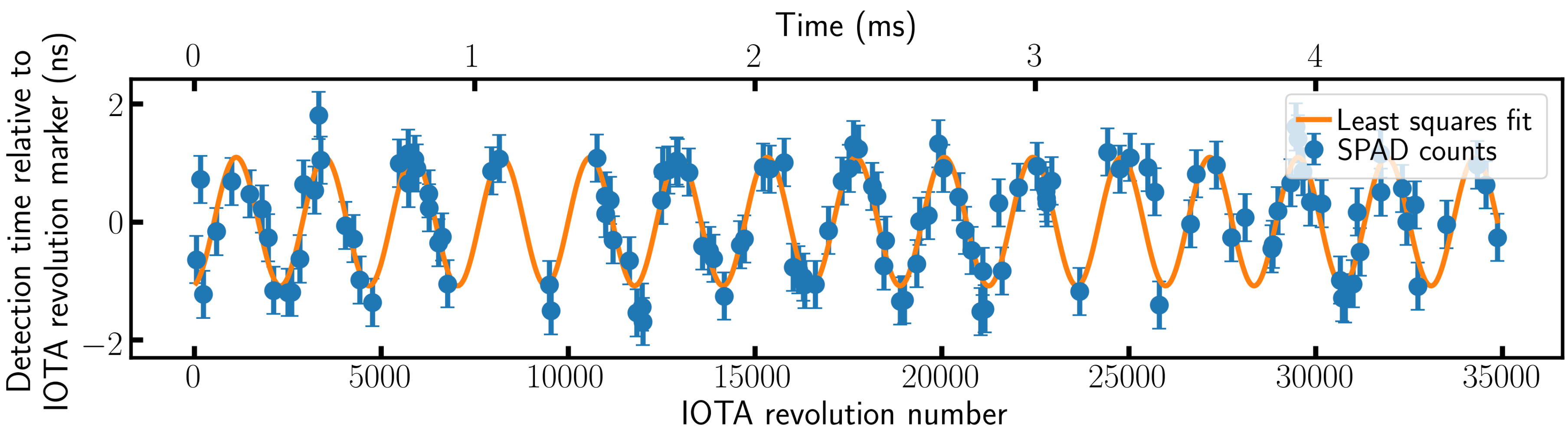

- The SPAD's timing resolution is ≈ 0.4 ns (the error bars)
- The outliers could also be the dark counts

Simulation of the single electron's synchrotron motion

Turn-by-turn map equations:

Radiation damping

Quantum excitation

$$\begin{cases} \delta_{i+1} = \delta_i + \dfrac{eV_0}{\beta^2 E_0}\left(\sin\phi_i - \sin\phi_s\right) - \dfrac{\langle U\rangle \mathcal{J}_E}{E_0}\delta_i - \dfrac{U_i - \langle U\rangle}{\beta^2 E_0} \\ \phi_{i+1} = \phi_i + 2\pi q \eta_s \delta_{i+1} + \xi_i \end{cases}$$

rf phase jitter (Gaussian)

$\eta_s = \alpha_c - 1/\gamma^2,$
$\alpha_c = 0.070\,86,$
$\eta_s = 0.070\,83,$
$V_0 = 380\,\mathrm{V},$
$\gamma = 188.6,$
$E_0 = 96.4\,\mathrm{MeV},$
$\phi_s = 0.0287\,\mathrm{rad},$
$\mathcal{J}_E = 2.64,$
$h = 4$

Average number of photons emitted per turn: $\langle N_\gamma \rangle = \dfrac{5\pi\alpha}{\sqrt{3}}\gamma = 12.5$ (mostly in bending magnets)

H. Burkhardt, "Monte Carlo generation of the energy spectrum of synchrotron radiation." http://cds.cern.ch/record/1038899/files/open-2007-018.pdf (2007)

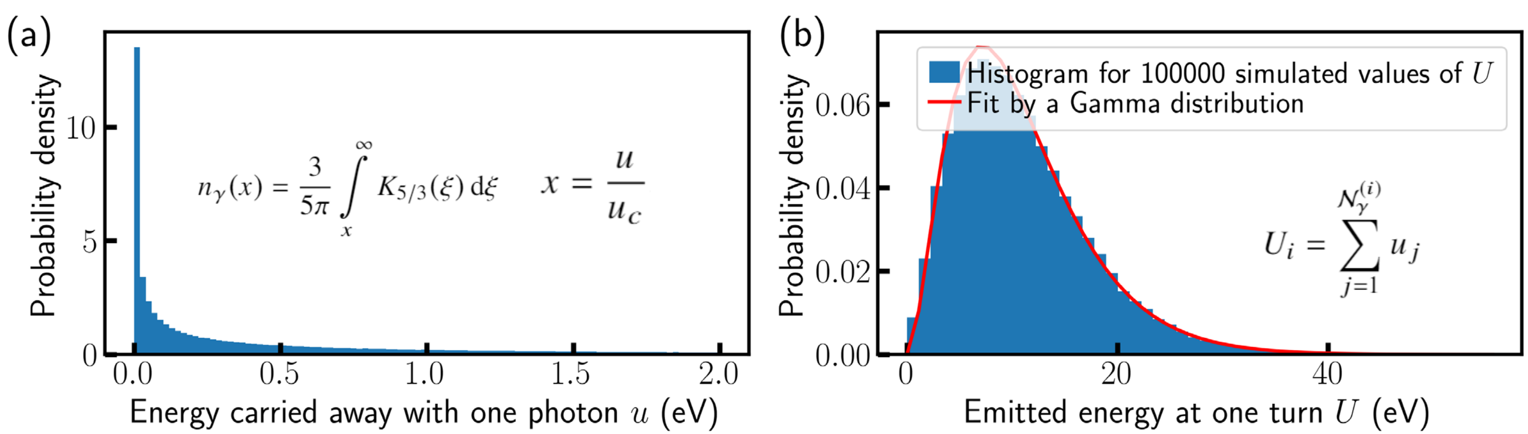

Fermilab

Synchrotron motion amplitude as a function of time

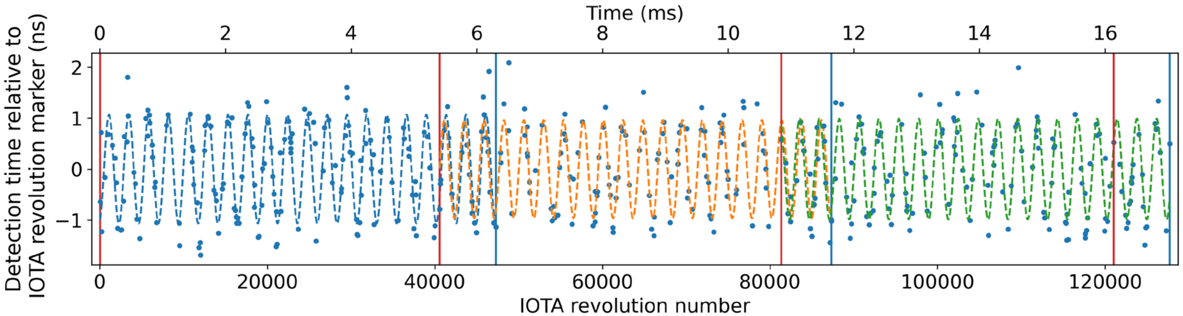

$A_1, A_2, A_3 \ldots$

The measurement and the simulation have similar behavior:

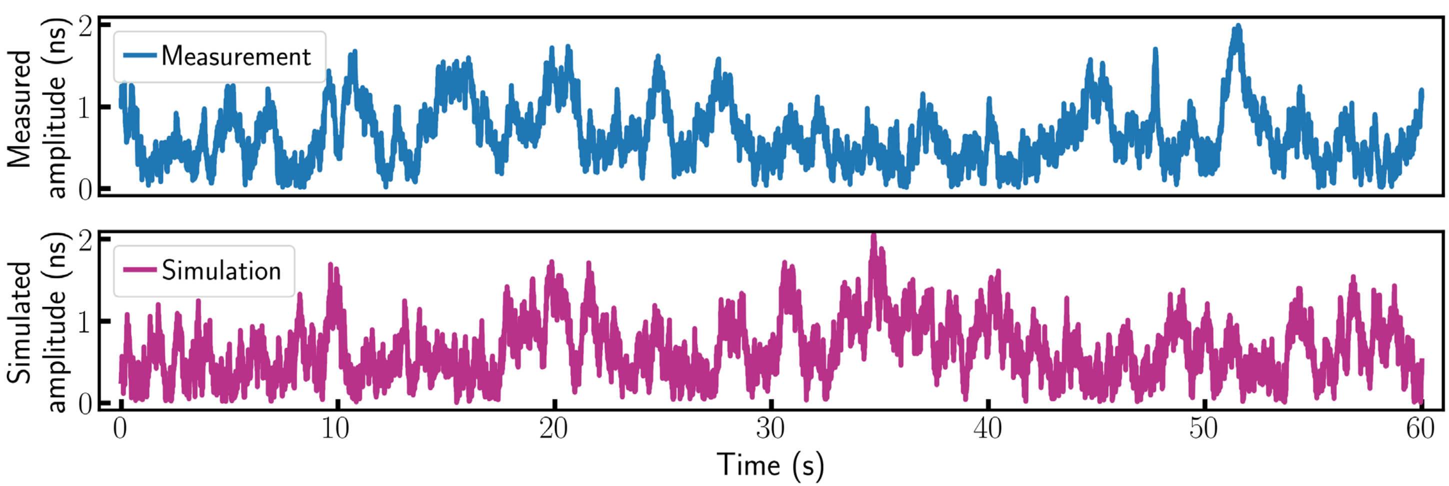

In this simulation, the rms phase jitter is

$$\sigma_\xi = 6 \times 10^{-5} \text{ rad}$$

Inference of the rms rf phase jitter

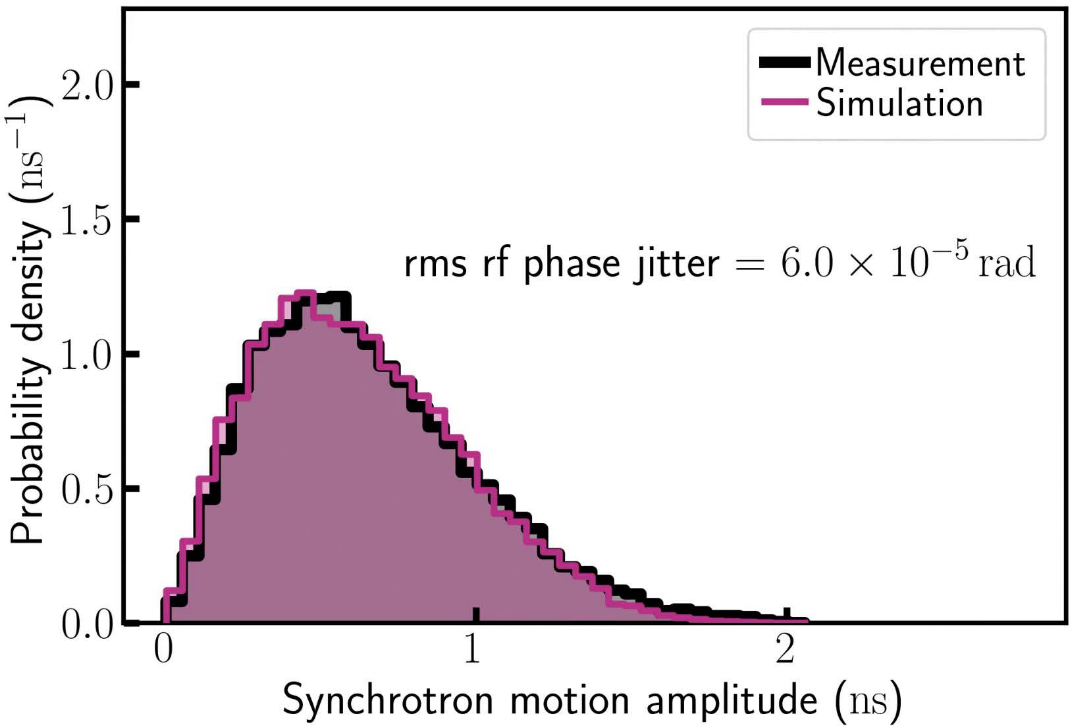

Journal of Instrumentation

PAPER • OPEN ACCESS

Single electron in a storage ring: a probe into the fundamental properties of synchrotron radiation and a powerful diagnostic tool

I. Lobach[1], S. Nagaitsev[1,2], A. Romanov[2] and G. Stancari[2]

Published 8 February 2022 • © 2022 The Author(s)

Journal of Instrumentation, Volume 17, February 2022

rms rf phase jitter

$$\sigma_\xi \approx 6 \times 10^{-5}\ \mathrm{rad}$$

$$\begin{cases} \delta_{i+1} = \delta_i + \dfrac{eV_0}{\beta^2 E_0}(\sin\phi_i - \sin\phi_s) - \dfrac{\langle U\rangle \mathcal{J}_E}{E_0}\delta_i - \dfrac{U_i - \langle U\rangle}{\beta^2 E_0} \\ \phi_{i+1} = \phi_i + 2\pi q \eta_s \delta_{i+1} + \xi_i \end{cases}$$

rf phase jitter

Here we use several data sets, the combined length is 150 seconds.

Synchrotron motion period as a function of amplitude

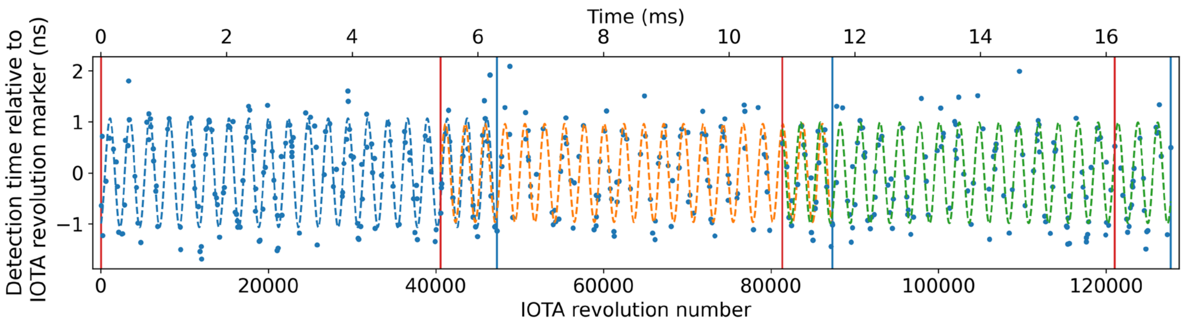

We can count the exact number of full synchrotron motion oscillations in a time interval

Thus, we can investigate sync. motion period as a function of amplitude:

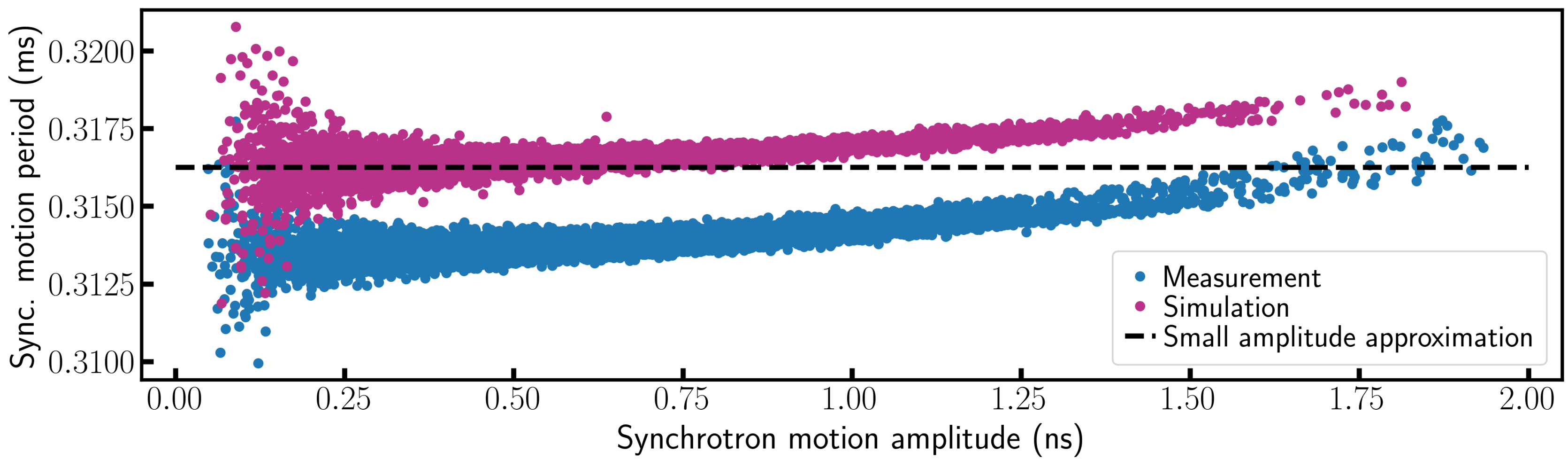

$$T_s = T_0\sqrt{\frac{2\pi E_0}{h\eta_s eV_0 \cos\phi_s}} = 0.3163\,\text{ms}$$

Each point corresponds to an estimation of the period in a time interval of **25 ms**

Effect of the detector's timing resolution

The distribution of residuals describes the
random delay introduced by the SPAD detector:

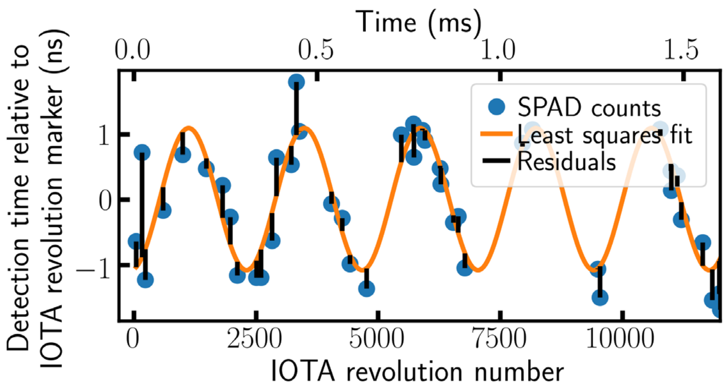

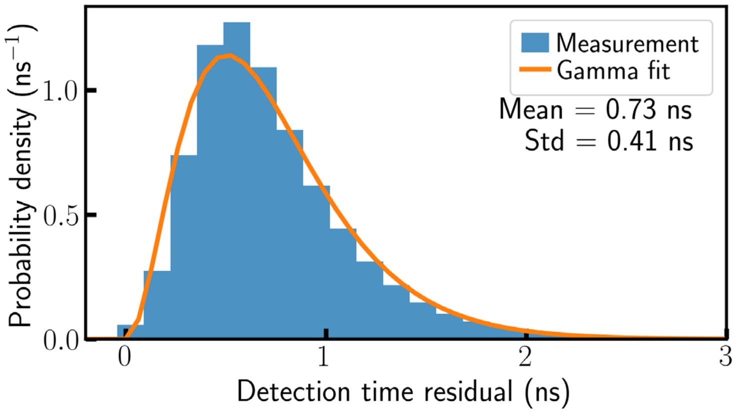

A real time video of the electron's longitudinal position with 0.1 sec-long "exposure":

(the residuals were removed)

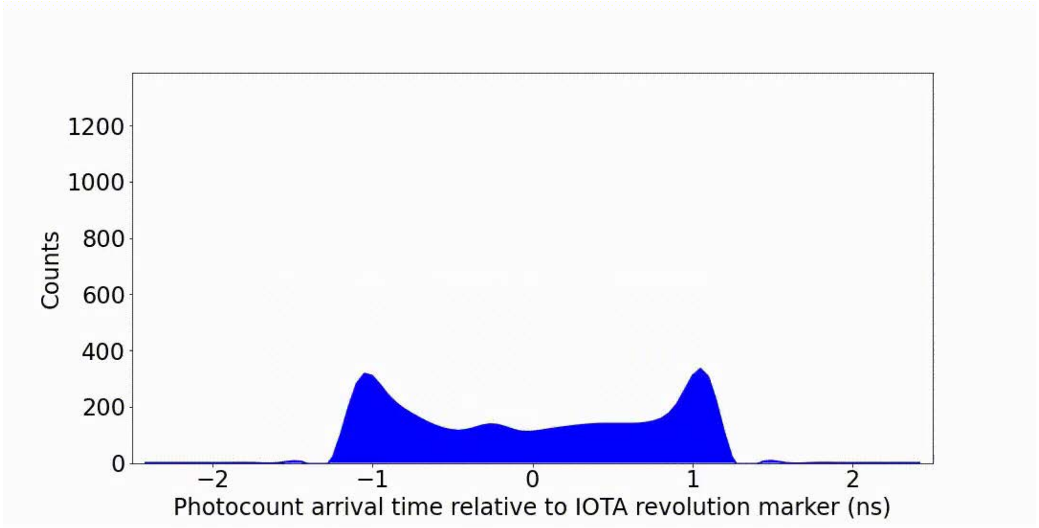

Fermilab

Thesis advisors:

Sergei Nagaitsev
(UChicago/Fermilab)

Giulio Stancari
(Fermilab)

IOTA team:

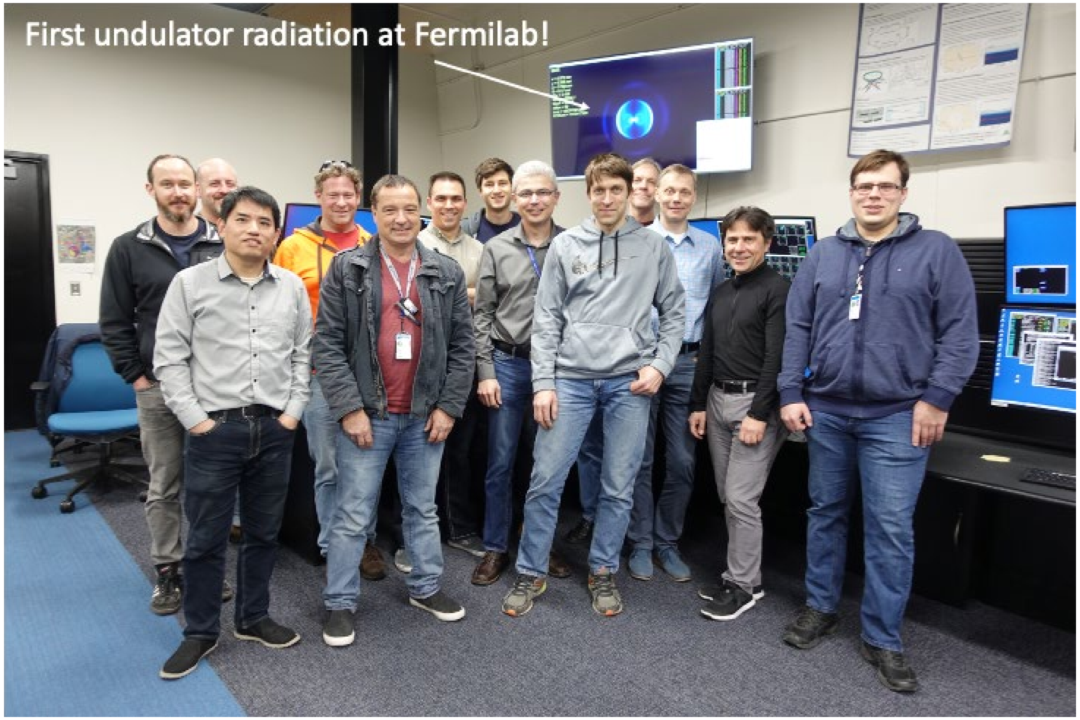

Aleksandr Romanov and Alexander Valishev tuned the ring and the beam. Mark Obrycki, James Santucci, Wayne Johnson, Dean Edstrom, and Kermit Carlson helped build the apparatus. Greg Saewert constructed the photodiode detection circuit and provided the test light source. Brian Fellenz, Daniil Frolov, David Johnson, and Todd Johnson provided some equipment and assisted during our detector tests. We had useful discussions about theoretical description with Valeri Lebedev and our collaborators from SLAC --- Aliaksei Halavanau and Zhirong Huang --- who also kindly provided the undulator.

Thank you for your attention!